RUSSIAN ACADEMY OF SCIENCE
Lenin Order of Siberian Branch
G.I. Budker INSTITUTE OF NUCLEAR PHYSICS

S.V. Miginsky

SPACE CHARGE EFFECT, COHERENCE OF CHARGE VIBRATION AND EMITTANCE

Novosibirsk
2007

Space charge effect,
coherence of charge vibration and emittance

S.V. Miginsky

Budker Institute of Nuclear Physics
630090, Novosibirsk, Russia

Abstract

Space charge effect is ever of fundamental importance for low-energy parts of accelerators. The technique known as emittance compensation allows analyzing and optimizing of this kind of beamlines effectively. Simple and robust estimations of the emittance degradation in various space charge affected beamlines and guns have been obtained analytically and numerically. Nonuniform longitudinal and transverse distributions of current, accelerating and bunching were taken into account. The parameters of optimal beamlines and guns for space charge affected beams have been estimated.

Эффект собственного заряда,
когерентность зарядовых колебаний и эмиттанс

С.В. Мигинский

Институт ядерной физики им. Г.И. Будкера
630090, Новосибирск, Россия

Аннотация

Эффект собственного заряда всегда играет важную роль в инжекторах ускорителей, где энергия частиц относительно невелика. Техника "emittance compensation" позволяет эффективно анализировать и оптимизировать такие каналы. В работе получены аналитически и численно простые и надежные оценки роста эмиттанса в каналах с превалирующим эффектом собственного заряда и пушках. Учитывались продольная и поперечная неоднородности плотности заряда, ускорение и группировка. Приведены оценки параметров оптимальных каналов и пушек.

1. Introduction

Space charge effect may cause significant emittance degradation in a beamline and even change the behavior of beam motion in a beamline. Kapchinsky-Vladimirsky equations [1] are very convenient to estimate the effect and also to analyze its results:

$$
\begin{cases}
a'' + k_x a - \dfrac{2j}{a+b} - \dfrac{\varepsilon_x^2}{a^3} = 0, \\[2mm]
b'' + k_y b - \dfrac{2j}{a+b} - \dfrac{\varepsilon_y^2}{b^3} = 0,
\end{cases}
\tag{1.1}
$$

where a and b are the envelopes in x an y directions; k is normalized focusing; $j = I/I_0 (\beta\gamma)^3$, normalized current; and ε is canonical emittance. We shall use the equations rewritten for rms-values

$$
\begin{cases}
x'' = \dfrac{\varepsilon_x^2}{x^3} + \dfrac{I}{I_0 (\beta\gamma)^3} \dfrac{1}{x+y} - \dfrac{e}{p} G_x x, \\[2mm]
y'' = \dfrac{\varepsilon_y^2}{y^3} + \dfrac{I}{I_0 (\beta\gamma)^3} \dfrac{1}{x+y} - \dfrac{e}{p} G_y y,
\end{cases}
\tag{1.2}
$$

where x and y mean horizontal and vertical rms-sizes and, in indexes, the appropriate coordinates respectively; $''$ means second derivative by the independent coordinate z; ε, I, G, e and p are the emittance, the current, the focusing gradient, the particle charge and its longitudinal momentum respectively. $I_0 = 4\pi \cdot mc^2/Z_0 e$, $\approx 17\,\text{kA}$ for electrons; $G_x = -G_y = G$ for a horizontally focusing quadrupole, $G_x = G_y = eB^2/4p$ for a solenoid, and $G_x = pg^2/e$, $G_y = 0$ for a dipole, where g is the trajectory curvature.

If the terms with current in (1.2) are comparable or greater than ones with emittance, one has to take into account space charge effect. So the following inequation is to be met to neglect space charge effect [2]:

$$
\frac{I}{I_0 (\beta\gamma)^3} \frac{1}{x+y} << \frac{\varepsilon_{x\,or\,y}^2}{(x \text{ or } y)^3},
\tag{1.3}
$$

3

Space charge also changes the phase of small vibration of a beam. If this is significant, one should estimate the effect before usage of a single-particle model. The equilibrium size of a beam is

$$x = \left(\frac{\varepsilon_x^2}{\frac{e}{p}G_x} + \frac{jx^3}{(x+y)\frac{e}{p}G_x} \right)^{1/4} \cong \left(\frac{\varepsilon_x^2}{\frac{e}{p}G_x} \right)^{1/4} \left(1 + \frac{1}{4}\frac{jx^3}{(x+y)\varepsilon_x^2} \right) \equiv x_0(1+\delta). \quad (1.4)$$

The equation of small vibration around this equilibrium is

$$\Delta x'' \cong -3\frac{\varepsilon_x^2}{x^4}\Delta x - \frac{j}{(x+y)^2}\Delta x - \frac{e}{p}G_x\Delta x. \quad (1.5)$$

Its wavenumber is

$$k^2 \cong 3\frac{\varepsilon_x^2}{x^4} + \frac{e}{p}G_x + \frac{j}{(x+y)^2} \cong 3\frac{\varepsilon_x^2}{x_0^4}(1-4\delta) + \frac{e}{p}G_x +$$

$$+ \frac{j}{(x+y)^2} = k_0^2 - 12\frac{\varepsilon_x^2}{x_0^4}\delta + \frac{j}{(x+y)^2}. \quad (1.6)$$

Space charge changes the wavenumber by

$$\Delta k \cong \frac{1}{2}\left(-12\frac{\varepsilon_x^2}{x_0^4}\delta + \frac{j}{(x+y)^2} \right) \Big/ k_0 = \frac{1}{2}\left(-\frac{3}{4}k_0\frac{jx^3}{(x+y)\varepsilon_x^2} + \frac{j}{(x+y)^2 k_0} \right) =$$

$$= \frac{1}{2}\left(-3\frac{j}{x(x+y)k_0} + \frac{j}{(x+y)^2 k_0} \right) = -\frac{1}{4}\frac{j(2x+3y)x}{\varepsilon_x(x+y)^2}. \quad (1.7)$$

$|(x-x_0)/x| \ll 1$ is assumed here. If $x \approx y$, than

$$\Delta k \cong -\frac{5}{16}\frac{j}{\varepsilon}. \quad (1.8)$$

Thus, the second ("phase") criterion of the validity of a single-particle model is

$$\frac{I}{4\varepsilon_x I_0(\beta\gamma)^3}\int \frac{j(2x+3y)x}{(x+y)^2}dz \ll 1, \quad (1.9)$$

A similar criterion for the vertical plane is obtained substituting $x \leftrightarrow y$. If $x \approx y$, one can simplify this condition

$$\frac{5}{16}\frac{I}{\varepsilon I_0(\beta\gamma)^3}L \ll 1, \quad (1.10)$$

where L is the total length of the beamline. One can also consider the betatron phase advance. The space charge effect is than

4

$$\Delta\varphi = \int\left(\frac{1}{\beta_0} - \frac{1}{\beta}\right)dz = \varepsilon_x \int\left(\frac{1}{x_0^2} - \frac{1}{x^2}\right)dz =$$

$$= 2\varepsilon_x \int\frac{\delta}{x^2 dz} = \frac{I}{2\varepsilon_x I_0(\beta\gamma)^3}\int\frac{x}{x+y}dz \approx \frac{I}{4\varepsilon I_0(\beta\gamma)^3}L. \tag{1.11}$$

Estimates (1.10) and (1.11) are very close.

Term "emittance compensation" was probably put forward in [3] in analysis of processes in RF photoelectron guns. Really, the author found that the normalized emittance oscillates along a gun due to space charge effect and the optimal phase advance can be chosen to minimize the emittance at the gun exit. The explanation was that the phase portraits of bunch slices diverge and converge periodically. The method was significantly formalized and developed in [4] and further works. Some of the results being discussed here have been presented in [5] - [7].

2. Basics

2.1. Longitudinal inhomogeneity: basic effect and equations

First of all, consider a bunch as a set of uniformly charged and independently moving slices with zero emittance. This is a good approximation if a bunch is long enough in the moving frame $\beta\gamma c\tau \gg r$. Substituting $I/I_0(\beta\gamma)^3 = j$, $G_x e/p = g$, $G_y e/p = h$ in (1.2) one obtains

$$\begin{cases} x'' = \dfrac{j}{x+y} - gx, \\ y'' = \dfrac{j}{x+y} - hy. \end{cases} \tag{2.1}$$

The longitudinal momentum and j are considered constant for the present. Suppose that $\begin{pmatrix} x \\ y \end{pmatrix}$ is a solution for the system (2.1), given j, and some starting conditions.

Let's name this solution as **principal**. Then the motion of another slice with the current $j + \delta j$ (all the values with δ are considered as small) is **homothetic** if its sizes are $\sqrt{\dfrac{j+\delta j}{j}}\begin{pmatrix} x \\ y \end{pmatrix} \cong \left(1 + \dfrac{1}{2}\dfrac{\delta j}{j}\right)\begin{pmatrix} x \\ y \end{pmatrix}$. It's obvious, as the substitution $j \to j + \delta j$, $\begin{pmatrix} x \\ y \end{pmatrix} \to \sqrt{\dfrac{j+\delta j}{j}}\begin{pmatrix} x \\ y \end{pmatrix}$ keeps (2.1) valid. This is the **principal** solution for the latter slice. Thus, the emittance of a bunch doesn't degrade if all its slices are homothetic. If one shapes a bunch in that way, the effect of longitudinal inhomogeneity is perfectly compensated.

If the starting conditions of the two mentioned slices are the same, the sizes of the second one will oscillate near the **principal** solution. The equations (linearized!) for a small deviation from the principal solution are then

$$\begin{cases} \delta x'' = -j\dfrac{\delta x + \delta y}{(x+y)^2} - g\delta x, \\[2mm] \delta y'' = -j\dfrac{\delta x + \delta y}{(x+y)^2} - h\delta y. \end{cases} \tag{2.2}$$

$\delta\begin{pmatrix} x \\ y \end{pmatrix} = -\dfrac{1}{2}\dfrac{\delta I}{I}\begin{pmatrix} x \\ y \end{pmatrix}$, $\delta\begin{pmatrix} x' \\ y' \end{pmatrix} = 0$ at $z = 0$. This is a system of linear equations with variable coefficients. Its local eigen solutions are

$$\left(-\dfrac{1}{\dfrac{\sqrt{(x+y)^4(g-h)^2+4j^2}+(x+y)^2(g-h)}{2j}} \right)\cdot\exp\left(\pm iz\sqrt{\dfrac{j}{(x+y)^2}+\dfrac{g+h}{2}-\sqrt{\dfrac{j^2}{(x+y)^4}+\left(\dfrac{g-h}{2}\right)^2}} \right),$$

$$\left(\dfrac{1}{\dfrac{\sqrt{(x+y)^4(g-h)^2+4j^2}-(x+y)^2(g-h)}{2j}} \right)\cdot\exp\left(\pm iz\sqrt{\dfrac{j}{(x+y)^2}+\dfrac{g+h}{2}+\sqrt{\dfrac{j^2}{(x+y)^4}+\left(\dfrac{g-h}{2}\right)^2}} \right). \tag{2.3}$$

In the case of axially symmetric focusing ($g = h > 0$) and quasistationary motion ($x = y$; $2j/(x+y)^2 = g$) these are a dipole mode and monopole one respectively Fig. 2.1:

$$\begin{pmatrix} 1 \\ -1 \end{pmatrix}\cdot\exp\left(\pm iz\dfrac{\sqrt{2j}}{x+y} \right),$$

$$\begin{pmatrix} 1 \\ 1 \end{pmatrix}\cdot\exp\left(\pm iz\dfrac{2\sqrt{j}}{x+y} \right). \tag{2.4}$$
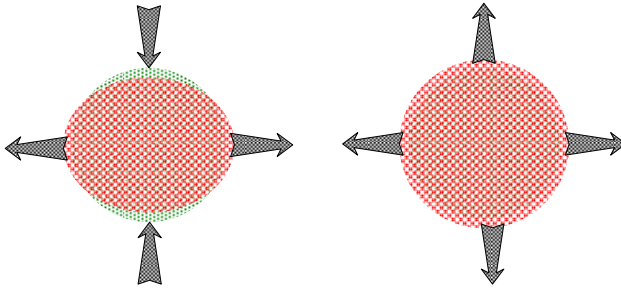
Fig. 2.1. Dipole (left) and monopole (right) charge vibration modes.

The wavenumber of the latter is $\sqrt{2}$ bigger. If both focusing and initial conditions are axially symmetric, the dipole mode is not excited and only the phase of the monopole mode (chare phase or phase for the sake of simplicity further) is to be $= \pi n$, where n is an integer to minimize the emittance. One can

6

say that small monopole vibrations of different slices are perfectly coherent so the phase portraits coincide periodically Fig. 2.2.
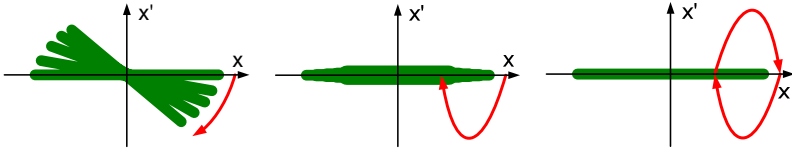
Fig. 2.2. Spread and narrowing of phase portraits of slices.

In the case of non-symmetrical motion both modes are to be phased that seems to be impossible.

2.2. Transverse inhomogeneity: basic effect and equations

The effect of transverse inhomogeneity is principal for steady beams and can affect significantly transient ones. Consider a slice of a transient beam or, that is similar, a steady beam with non-uniform transverse charge distribution. Let's assume the whole system as axially symmetric. Then the equation for a particle at a distance x from the axis is

$$x'' = \frac{\widetilde{I}}{I_0(\beta\gamma)^3}\frac{2}{x} - gx = \frac{2\widetilde{j}}{x} - gx, \tag{2.5}$$

where $\widetilde{I}$ is the current inside a cylinder of radius x, and all other symbols are as in (2.1). Let's suppose that the motion is perfectly laminar, that is if $x_1 > x_2$ for two particles at some place, it is valid everywhere. This condition is not always valid, but is violated only in the low-density halo of a beam, so almost doesn't affect estimation of emittance.

If the charge distribution of a beam (slice) is not uniform, $\widetilde{j}$ is not proportional to x^2, and particle trajectories are not **homothetic**. The situation looks like in Fig. 2.3.
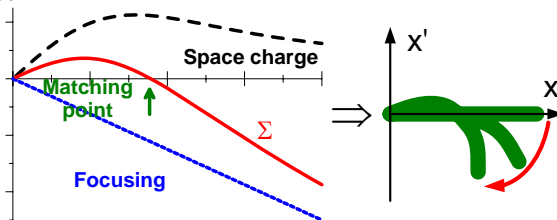
Fig. 2.3. Motion of Gaussian slice.

Similar to the case of longitudinal inhomogeneity, one can consider a set of **homothetic principle** trajectories for different particles and their oscillations around the trajectories. The linearized equation for small deviation is then

$$\delta x'' = -\left(\frac{2\tilde{j}}{x^2} + g\right)\delta x. \tag{2.6}$$

In the linear approximation, the phase portrait of a slice is straightened twice per a period of oscillation and the emittance is zeroed.

If there is Gaussian distribution of current within a slice of the rms-size r and current j, then

$$\tilde{j}(x) = \int_0^x \frac{j}{2\pi r^2} 2\pi r \exp\left(\frac{-x^2}{2r^2}\right) dx = j\left(1 - \exp\left(\frac{-x^2}{2r^2}\right)\right). \tag{2.7}$$

Wavenumbers of oscillations of a slice in total and a particle inside it coincide if
$1 - \exp\left(-x^2/2r^2\right) = x^2/2r^2 \Rightarrow x \cong 1.7852866r$.

2.3. General dimensionless equations of small oscillations

It is more convenient to analyze a dimensionless deviation $\delta = \delta x / x$. If a round beam is uniform in the transverse plane and its energy and current are conserved, its rms-size is given by

$$x'' = \frac{j}{2x} - gx. \tag{2.8}$$

For a small deviation δ from the principle trajectory, the linearized equation is then

$$(x(1+\delta))'' = \frac{j}{2x(1+\delta)} - gx(1+\delta) \Rightarrow \delta'' + 2\frac{x'}{x}\delta' = -\frac{j}{x^2}\delta. \tag{2.9}$$

If the energy and/or the current are variable, the equation for the rms-size is

$$\begin{cases} x' = \dfrac{x_1}{\beta\gamma} \\ x_1' = \beta\gamma\left(\dfrac{j}{2x} - gx\right) \end{cases} \Rightarrow x'' + \frac{(\beta\gamma)'}{\beta\gamma}x' = \frac{j}{2x} - gx, \tag{2.10}$$

where $x_1 = \beta\gamma x'$ is the normalized slope. The linearized equation for a small deviation is then

$$\delta'' + \left(2\frac{x'}{x} + \frac{(\beta\gamma)'}{\beta\gamma}\right)\delta' = -\frac{j}{x^2}\delta. \tag{2.11}$$

Note that the coefficient at δ in the right part is ever negative, that is the motion is ever stable, and doesn't depend explicitly on the focusing. All the principle trajectories are homothetic, that is $x_1'/x_1 = x_2'/x_2$ for any two of them. So the phase portraits of the slices are aligned if

$$\frac{x_1' + \delta x_1'}{x_1 + \delta x_1} = \frac{x_2' + \delta x_2'}{x_2 + \delta x_2}. \tag{2.12}$$

Considering terms with δ as small one obtains

$$\delta_1' = \delta_2'. \tag{2.13}$$

Property $\delta x' = x\delta' + x'\delta x / x$ has been used here. Consider the situation in more details. Assume that some slice moves along the principle trajectory (x_0, x_0'). Adjacent slices have principal trajectories $\xi \cdot (x_0, x_0')$, where ξ is a parameter, and deviations $(\xi - 1)(\delta x_0, \delta x_0')$, that are small. Applying (2.13) to all the slices one obtains (Fig. 2.4)

$$\delta_0' = 0 \Leftrightarrow \delta x / x = \delta x' / x'. \tag{2.14}$$

Thus, it is necessary to find the points where $\delta' = 0$ to minimize emittance.
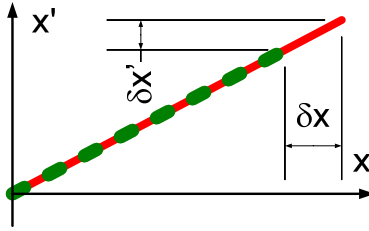
Fig. 2.4. Alignment of phase portraits.

One should substitute $j \leftarrow 4\tilde{j}$ in (2.11) to obtain the appropriate equation for the effect of transverse inhomogeneity

$$\delta'' + \left(2\frac{x'}{x} + \frac{(\beta\gamma)'}{\beta\gamma}\right)\delta' = -\frac{4\tilde{j}}{x^2}\delta. \tag{2.15}$$

2.4. Transformation matrix and phase

As any linear ordinary differential equation (ODE) of the second order, (2.11) (also (2.15)) defines the transformation matrix between two arbitrary points of a beamline z_0 and z_1

$$\mathbf{M}(z_0, z_1) = \begin{pmatrix} C & S \\ C' & S' \end{pmatrix}, \tag{2.16}$$

where (C, C') and (S, S') are the values of (δ, δ') at z_1, if at z_0 they were $(1, 0)$ and $(0, 1)$ respectively. They are well-known cos- and sin-like trajectories. In general, the coefficient at δ' in (2.11) and (2.15) is not zero, so $\det \mathbf{M}$ is not necessary unity [8]

$$\det \mathbf{M}(z_0, z_1) = \exp\left(-\int_{z_0}^{z_1}\left(2\frac{x'}{x} + \frac{(\beta\gamma)'}{\beta\gamma}\right)dz\right) = \left(\frac{x_0}{x_1}\right)^2\frac{(\beta\gamma)_0}{(\beta\gamma)_1}.$$ (2.17)

The transformation matrix of a uniform beamline with x and $\beta\gamma$ = const is

$$\mathbf{M}(z_0, z_1) = \begin{pmatrix} \cos\varphi & \dfrac{x}{\sqrt{j}}\sin\varphi \\[2mm] -\dfrac{\sqrt{j}}{x}\sin\varphi & \cos\varphi \end{pmatrix},$$ (2.18)

where $\varphi = (z_1 - z_0)\sqrt{j}/x$. One can obtain the inverse matrix substituting $\varphi \to -\varphi$. Probably, this is the only case when the charge phase advance can be defined absolutely correctly, that is the phase advances of two parts are (i) additive and (ii) commutative. Nevertheless, we are interesting in cos-like trajectories most of all ($\delta' = 0$ in the birth-place of a beam), so the phase advance of a beamline can be defined by equating it with the "appropriate" uniform beamline. A uniform beamline is appropriate to the given one if the values x, j and $\beta\gamma$ in the former and at the **end** of the latter are equal and the ratio of C and C' elements of the transformation matrices and their signs coincide. In this case the phase advance in the beamline is

$$\varphi = \arctan\left(\frac{-C'x}{C\sqrt{j}}\right),$$ (2.19)

where the quadrant is selected so that the signs of $\cos\varphi$ and $-\sin\varphi$ coincide to the ones of C and C' respectively. This phase is not ever additive and commutative, but gives an idea on the most important beamline parameters and possesses several useful properties. If a uniform beamline with the phase advance $\pi - \varphi$ is added to the end of an arbitrary one with the phase advance φ, and x, j and $\beta\gamma$ in the former and at the **end** of the latter are equal, then the total phase advance of the combined beamline is π:

$$\begin{pmatrix} \cos(\pi - \varphi) & \dfrac{x}{\sqrt{j}}\sin(\pi - \varphi) \\[2mm] -\dfrac{\sqrt{j}}{x}\sin(\pi - \varphi) & \cos(\pi - \varphi) \end{pmatrix}\cdot\begin{pmatrix} a\cos\varphi & * \\[2mm] -a\dfrac{\sqrt{j}}{x}\sin\varphi & * \end{pmatrix} = \begin{pmatrix} -a & * \\ 0 & * \end{pmatrix}.$$ (2.20)

The analogous situation occurs for addition $2\pi - \varphi$. A set of beamlines with the phase advances divisible by π has the phase advance also divisible by π. It follows from the fact that the product of two superdiagonal matrices is also a superdiagonal matrix

$$\begin{pmatrix} * & * \\ 0 & * \end{pmatrix}\cdot\begin{pmatrix} * & * \\ 0 & * \end{pmatrix} = \begin{pmatrix} * & * \\ 0 & * \end{pmatrix}.$$ (2.21)

Moreover, if the number of the parts the with phase advance π is odd, the total phase advance is π, otherwise it is 2π. It is due to the resulting C is the product of C of partial matrices. Of course, x, j and $\beta\gamma$ at the end of the previous part and the beginning of the next one must be equal.

It must be emphasized that (i) the mentioned **charge vibration phase is not the same as the well-known betatron phase**. The analogy is only due to the same type of the generating equations. Further, (ii) its definition (2.19) is proper for analysis of emittance compensation, but is not solely possible.

3. Beamlines

3.1. Uniform beamline: longitudinal inhomogeneity

Let's estimate emittance dilution owing to the longitudinal inhomogeneity effect in a uniform axially symmetric beamline with constant energy and current. Apparently, this is the simplest case. The matter is that only small oscillation is linear that is harmonic, but if the amplitude is not zero, the wavenumber of this oscillation differs from the harmonic one. It disturbs the coherence of the different slices. The linearized equation (2.11) gives the same phase for all the slices, so we need to use next approximations

$$\delta'' + \frac{j}{x^2}\delta = \frac{j}{2x^2}\delta^2 - \frac{j}{2x^2}\delta^3 \Leftrightarrow \delta'' + 2g\delta = g\delta^2 - g\delta^3, \tag{3.1}$$

where terms higher than cubic were omitted. An analogous equation was analyzed in [9] (28,9)

$$\ddot{x} + \omega_0^2 x = -\alpha x^2 - \beta x^3, \tag{3.2}$$

and the frequency shift due to nonlinearity was found (28,13)

$$\omega^{(2)} = \left(\frac{3\beta}{8\omega_0} - \frac{5\alpha^2}{12\omega_0^3}\right)a^2, \tag{3.3}$$

where a is the amplitude. In our case

$$\omega_0 = \sqrt{2g}, \alpha = -g, \beta = g. \tag{3.4}$$

Substituting (3.4) into (3.3) one obtains

$$\frac{\omega^{(2)}}{\omega_0} = \frac{1}{12}a^2. \tag{3.5}$$

Thus, the linearly increasing phase shift is

$$\Delta\varphi \cong \frac{1}{12}\varphi a^2, \tag{3.6}$$

where φ is the total phase advance. Consider a bunch emitted with equal $x = r$ and zero x' for all the slices and having Gaussian distribution of current along the

longitudinal axis:
$$j = j_0 \exp(-\varsigma^2) . \tag{3.7}$$

Let the stationary condition $j_0 \exp(-\varsigma_0^2) = 2r^2 g$ is valid for some slice at ς_0, and its phase advance through the beamline $\sqrt{2g}L = 2\pi n$, where n is integer. Then the sizes of all the neighbour slices at the end are approximately equal and their phases are not equal due to the effect of the cubic (and higher) terms in (3.1). The principal size (also stationary) of any slice is
$$x_S = r \exp\left(\left(\varsigma_0^2 - \varsigma^2\right)/2\right), \tag{3.8}$$

and the relative charge vibration amplitude is
$$a = (r - x_S)/x_S = \exp\left(\left(\varsigma^2 - \varsigma_0^2\right)/2\right) - 1 . \tag{3.9}$$

At the end of the beamline
$$x' = x_S \delta' + x_S'(1+\delta) \cong -a x_S \sqrt{2g}\Delta\varphi \cong -\frac{1}{12}\varphi a^3 x_S \sqrt{2g} =$$
$$= -\frac{1}{12}\varphi r \sqrt{2g} \exp\left(\varsigma^2 - \varsigma_0^2\right)\left(1 - \exp\left(\left(\varsigma_0^2 - \varsigma^2\right)/2\right)\right)^3 . \tag{3.10}$$

If one substitutes this expression into the integrals for $<x'^2>$ and $<xx'>$, they diverge. x' in

(3.10) grows exponentially with ς, while in fact $|x'| < r\sqrt{2g}\left(1 - \exp\left(\left(\varsigma_0^2 - \varsigma^2\right)/2\right)\right)$. So let's bound x' as

$$x' \cong \frac{1}{2}r\sqrt{2g}\left(1 - \cos\left(\sqrt{\frac{\varphi}{12}}\left(\varsigma^2 - \varsigma_0^2\right)\right)\right)\left(1 - \exp\left(\left(\varsigma_0^2 - \varsigma^2\right)/2\right)\right). \tag{3.11}$$

The lowest terms of the series expansions of both expressions at zero by $\left(\varsigma_0^2 - \varsigma^2\right)$ coincide. Emittance is calculated as
$$<x^2> = x^2,$$
$$<x'^2> = \int_0^\infty x'^2 \exp(-\varsigma^2)d\varsigma \left/ \int_0^\infty \exp(-\varsigma^2)d\varsigma, \right.$$
$$<xx'> = \int_0^\infty xx' \exp(-\varsigma^2)d\varsigma \left/ \int_0^\infty \exp(-\varsigma^2)d\varsigma, \right. \tag{3.12}$$
$$\varepsilon_x = \sqrt{<x^2><x'^2> - <xx'>^2} .$$

Final expressions are bulk enough, so are not placed here. ε and optimal ς_0 for $j = 1$, $r = 1$, and n from 1 to 15 are placed in Fig. 3.1.

12
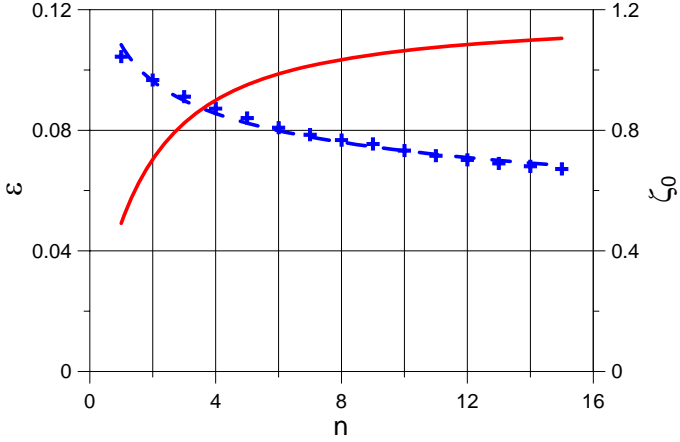
Fig. 3.1. ε (red solid) and ς_0 (blue crosses) vs. number of periods. Blue dashed is $1.084n^{-0.170}$.

The emittance grows with n from 0.049 up to the asymptotic value 0.12. Optimal $\varsigma_0 \approx 1.084n^{-0.170}$. Thus, in the first 2π-minimum

$$\varepsilon \approx 0.049r\sqrt{j} , \tag{3.13}$$

and it grows up to

$$\varepsilon \approx 0.12r\sqrt{j} , \tag{3.14}$$

when $n \to \infty$. Every time g is optimal for given n and approximately equals to $j\exp(-1.175n^{-0.340})/2x^2$.

Let's estimate this effect if the phase is not optimal. Then assume the phase portraits of the slices, except of ς_0, uniformly distributed over ellipses

$$\begin{aligned} x &= r\big(\exp\big((\varsigma_0^2 - \varsigma^2)/2\big)+\cos\psi\big(1-\exp\big((\varsigma_0^2 - \varsigma^2)/2\big)\big)\big), \\ x' &= r\sqrt{2g}\,\sin\psi\big(1-\exp\big((\varsigma_0^2 - \varsigma^2)/2\big)\big), \end{aligned} \tag{3.15}$$

where ψ is the arbitrary phase. For each slice

$$<\widetilde{x}^2> = \frac{r^2}{2\pi}\int_0^{2\pi}\big(\exp\big((\varsigma_0^2 - \varsigma^2)/2\big)+\cos\psi\big(1-\exp\big((\varsigma_0^2 - \varsigma^2)/2\big)\big)\big)^2 d\psi =$$

$$= \frac{r^2}{2}\big(1-2\exp\big((\varsigma_0^2 - \varsigma^2)/2\big)+3\big(\exp\big((\varsigma_0^2 - \varsigma^2)/2\big)\big)^2\big), \tag{3.16}$$

$$<\widetilde{x}'^2> = \frac{r^2 g}{\pi}\int_0^{2\pi}\big(\sin\psi\big(1-\exp\big((\varsigma_0^2 - \varsigma^2)/2\big)\big)\big)^2 d\psi = r^2 g\big(1-\exp\big((\varsigma_0^2 - \varsigma^2)/2\big)\big)^2,$$

$$<\widetilde{x}\widetilde{x}'> = 0.$$

13

For the total bunch

$$<x^2> = \frac{2}{\sqrt{\pi}}\int_0^\infty <\tilde{x}^2> \exp(-\varsigma^2)d\varsigma = r^2\left(\frac{1}{2} - \frac{\sqrt{6}}{3}\exp(\varsigma_0^2/2) + \frac{3\sqrt{2}}{4}\exp(\varsigma_0^2)\right),$$

$$<x'^2> = \frac{2}{\sqrt{\pi}}\int_0^\infty <\tilde{x}'^2> \exp(-\varsigma^2)d\varsigma = 2gr^2\left(\frac{1}{2} - \frac{\sqrt{6}}{3}\exp(\varsigma_0^2/2) + \frac{\sqrt{2}}{4}\exp(\varsigma_0^2)\right), \qquad (3.17)$$

$$\varepsilon_x = \sqrt{<x^2><x'^2>}.$$

ε_x reaches the minimum at $\varsigma_0 \cong 0.540$, the value is ≈ 0.144 if $j = 1$ and $x = 1$. Thus, if the phase is not optimized, the emittance can be

$$\varepsilon \approx 0.144 r\sqrt{j}, \qquad (3.18)$$

that is triple larger than in the 2π-minimum.

Let's verify these estimations numerically now. Code "Butterfly" has been developed for this purpose. The code simulates the motion of an axially symmetric bunch with uniform charge distribution in the transverse plane and Gaussian one along the longitudinal axis through an axially symmetric uniform beamline. The motion equation

$$x'' = \frac{j}{2x} - gx \qquad (3.19)$$

derived from (2.1) is solved by Dormand-Prince 5(4) scheme [10] within $0 < z < 100$ for each slice independently. Initial data are ever $x = 1$, $x' = 0$, the peak current is ever 1, g is varied. Dense output of x and x' with the step 0.05 is performed. The emittance and the rms-size of the bunch are calculated using these data in the nodes of the mentioned grid. Necessary mean values are ever calculated as

$$<\xi> = \frac{2}{\sqrt{\pi}}\int_0^1 \xi\left(\frac{\vartheta}{1-\vartheta}\right)\exp\left(-\left(\frac{\vartheta}{1-\vartheta}\right)^2\right)\frac{d\vartheta}{(1-\vartheta)^2} \qquad (3.20)$$

to avoid the infinity limits in the integrals. Change of variable $\varsigma = \vartheta/(1-\vartheta)$ is used for this purpose. The integrand is limited within the mentioned limits, so no problems with numerical integration occur. The integrals are calculated with code "DLobatto" described in [11] and [12].

Problems occur when slices carrying small currents pass waists. For example, the minimal radius of a slice with the current 0.0183 ($\varsigma = 2$) in $g = 0.168$ ($\varsigma_0 = 1.044$, the optimum for the 2π-minimum) is

$$x_c = \exp(-g/j) \approx 10^{-4}, \qquad (3.21)$$

so the integration step must be too small $\sim x_c$ and the integration procedure is ineffective. As a bunch ever contains small-current slices, the problem ever occurs. To solve it, consider the canonical form of (3.19). Its Hamiltonian is

$$H = \frac{p^2}{2} - \frac{j}{2}\ln x + \frac{g}{2}x^2, p \equiv x' \ . \tag{3.22}$$

Of course, it preserves. Then the order of the equation can be reduced

$$\frac{x'^2}{2} - \frac{j}{2}\ln x + \frac{g}{2}x^2 = H_0 \ . \tag{3.23}$$

In a crossover

$$x_c = x_0 \exp\left(- x_0'^2 / j\right). \tag{3.24}$$

The advance of z in passing it from (x_0, x'_0) to $(x_0, -x'_0)$ is

$$\Delta z = 2\int_{x_c}^{x_0} \frac{d\chi}{\sqrt{j \ln(\chi/x_0) + x_0'^2}} \ . \tag{3.25}$$

Unfortunately, the integrand has an integrable singularity at the lower limit. Let's substitute $\xi^2 = \chi - x_c$ to avoid it:

$$\Delta z = 4 \int_0^{\sqrt{x_0 - x_c}} \frac{\xi d\xi}{\sqrt{j \ln\left((\xi^2 + x_c)/x_0\right) + x_0'^2}} \ . \tag{3.26}$$

The integrand is limited within the integration limits and its value at the lower one is

$$\sqrt{\frac{x_0}{j} \exp\left(-\frac{x_0'^2}{j} \right)} \ . \tag{3.27}$$

This value must be used if

$$\frac{1}{4}\frac{\xi^2}{x_0} \exp\left(\frac{x_0'^2}{j} \right) < Tol \ , \tag{3.28}$$

where *Tol* is the claimed accuracy. The same "DLobatto" code is used here. Calculated Δz is added to z, x' is inverted, and the integration procedure goes on. If a node of the dense output grid occurs at the crossover, its value is calculated from the interpolation polynomial of the next integration step.

The integrator can ignore a crossover as the right part is evaluated only in a few nodes within a step. In this case the transition doesn't affect the accuracy. The sign of x is ever checked and, if necessary, inverted together with the one of x'.

Let's examine numerical results. Analytical estimation above yields the optimal $\varsigma_0 = 1.044$ and the focusing $g = 0.5\exp(-\varsigma_0^2) \cong 0.168$ for 2π-minimum. The results for this case are placed in Fig. 3.2. First $2\pi n$-minimum of the emittance occurs at $z \approx 10.6$ ($\varphi = \sqrt{2gz} \approx 1.96\pi$), and its value is $\varepsilon \approx 0.036$. The analytical result is $\varepsilon \approx 0.049$ at $z \approx 10.84$. It was found that the optimal g for 2π-minimum in

the numerical model is ≈ 0.09 ($\varsigma_0 \approx 1.310$). The results for this case are placed in Fig. 3.3. First $2\pi n$-minimum of the emittance occurs in this case at $z \approx 14.2$ ($\varphi = \sqrt{2gz} \approx 1.92\pi$), its value is $\varepsilon \approx 0.023$. An obvious difference between the two cases is that the values in $2\pi n$-minima differ not so much in the former (it corresponds well to Fig. 3.1), while they increase almost linearly with n in the latter. In both cases values in $(2n+1)\pi$-minima are bigger than in $2\pi n$ ones. At lower g the beats of ε and the rms-size increase and ε in minima increases too.
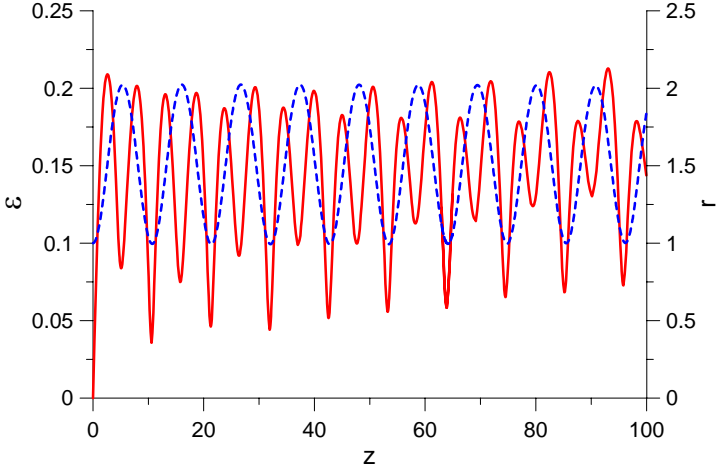
Fig. 3.2. ε (red solid) and rms-size (blue dashed) of a bunch in g = 0.168.
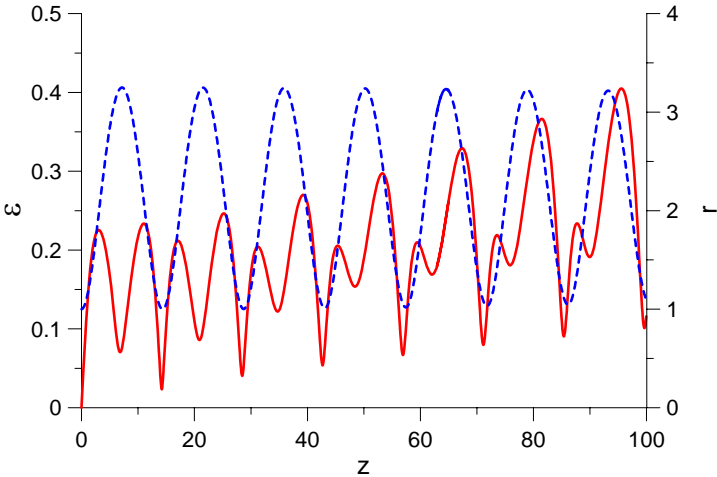
Fig. 3.3. ε (red solid) and rms-size (blue dashed) of a bunch in g = 0.09.

Optimal parameters for maxima are $\varsigma_0 = 0.540$ and $g = 0.5\exp(-\varsigma_0^2) \cong 0.374$. The results for this case are placed in Fig. 3.4.
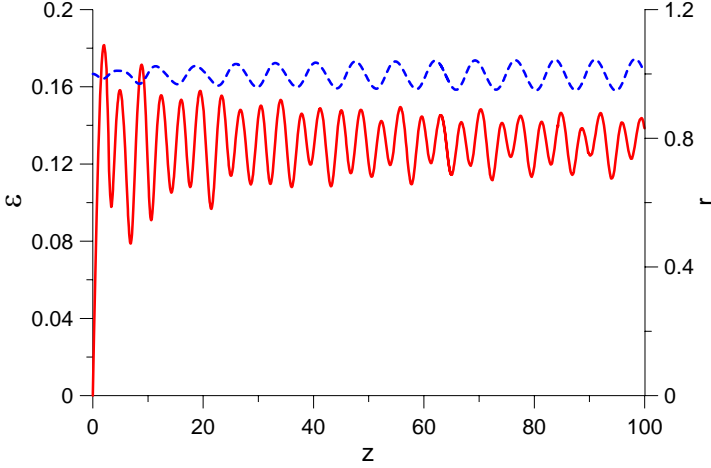
Fig. 3.4. ε (red solid) and rms-size (blue dashed) of a bunch in g = 0.374.

One can see the size beating is small enough, that is the focusing is near matched ($g \approx 0.40$ gives a little lower beating). The emittance beating is also small. Its value in all the maxima except of first and third ones is ≈ 0.15. The analytical estimate (3.18) gives 0.144 that is in good agreement.

It should be mentioned also that $g = 0.2\ldots0.3$ are optimal for $2\pi n$-minima with large n. The typical minimal value is $\varepsilon \approx 0.07$. The analytical estimate Fig. 3.1, (3.14) gives $\varepsilon \approx 0.12$ and $g \approx 0.3$.

Thus, the derived analytical estimate is verified in toto by numerical experiments. The optimal numerical emittance value in the 2π-minimum is significantly lower than the analytical one and the optimal focusing is weaker. The analytical result for $2\pi n$-minima is valid while the focusing is overestimated a little. For maxima, the estimate is in good agreement with the numerical results.

3.2. Uniform beamline: transverse inhomogeneity

Let's estimate the effect of transverse inhomogeneity now. Consider Gaussian transverse distribution with the current j and the rms-size r. The beam moves through a uniform beamline with focusing g. The initial radius of a particle is y and $y' = 0$. Then

$$\tilde{j} = j\left(1 - \exp\left(-y^2/2r^2\right)\right) \tag{3.29}$$

and, if $gr^2/j < 1$, an immovable particle exists, which radius x_0 satisfies the equation

17

$$\left(1 - \exp\left(- x_0^2 / 2r^2\right)\right)/x_0^2 = g/2j .$$ (3.30)

The principal (equilibrium) radius of another particle is

$$x_e = \sqrt{\frac{2j\left(1 - \exp\left(- y^2 / 2r^2\right)\right)}{g}} .$$ (3.31)

The relative charge vibration amplitude is

$$a = \frac{\left(y - x_e\right)}{x_e} = \frac{y}{x_0}\sqrt{\frac{1 - \exp\left(- x_0^2 / 2r^2\right)}{1 - \exp\left(- y^2 / 2r^2\right)}} - 1.$$ (3.32)

In $2\pi n$-minima the transverse coordinate of a particle and its derivative are

$$x \cong y ,$$ (3.33)

$$x' \cong -ax_e\sqrt{2g}\Delta\varphi \cong$$

$$\cong \frac{1}{12}\varphi\sqrt{2g}\,x_0\sqrt{\frac{1 - \exp\left(- y^2 / 2r^2\right)}{1 - \exp\left(- x_0^2 / 2r^2\right)}}\left(\frac{y}{x_0}\sqrt{\frac{1 - \exp\left(- x_0^2 / 2r^2\right)}{1 - \exp\left(- y^2 / 2r^2\right)}} - 1\right)^3 .$$ (3.34)

Dephasing here is because of the same nonlinearity as in the above case. Average values necessary for the emittance are

$$< x^2 >= r^2 ,$$ (3.35)

$$< x'^2 >= \frac{1}{2r^2}\int_0^\infty x'^2 y \exp\left(- y^2 / 2r^2\right)dy \cong$$

$$\cong \frac{1}{288}\varphi^2 j\left(57.69873135\frac{r^4}{x_0^4}\left(1 - \exp\left(- x_0^2 / 2r^2\right)\right)^2 + \right.$$

$$+144.2468283\frac{r^2}{x_0^2}\left(1 - \exp\left(- x_0^2 / 2r^2\right)\right)+ 30 + \frac{1}{2}\frac{x_0^2}{r^2}\frac{1}{1 - \exp\left(- x_0^2 / 2r^2\right)}$$

$$-5.879821772\frac{x_0}{r}\frac{1}{\sqrt{1 - \exp\left(- x_0^2 / 2r^2\right)}} -$$

$$-85.48606633\frac{r}{x_0}\sqrt{1 - \exp\left(- x_0^2 / 2r^2\right)} -$$

$$\left. -137.2523488\frac{r^3}{x_0^3}\left(1 - \exp\left(- x_0^2 / 2r^2\right)\right)^{3/2}\right),$$ (3.36)

$$<xx'> = \frac{1}{2r^2}\int\limits_0^\infty x'y^2\exp\left(-y^2/2r^2\right)dy \cong \frac{1}{24}\varphi r\sqrt{j}\times$$

$$\times\left(-0.9799702953\frac{x_0}{r}\frac{1}{\sqrt{1-\exp\left(-x_0^2/2r^2\right)}}+\right.$$

$$+6-12.82290995\frac{r}{x_0}\sqrt{1-\exp\left(-x_0^2/2r^2\right)}$$

$$\left.+9.616455226\frac{r^2}{x_0^2}\left(1-\exp\left(-x_0^2/2r^2\right)\right)\right)$$

(3.37)

The expression for the emittance is too bulk to place it here. The emittance gets the minimum at $x_0 \approx 2.292r$, that is the optimal focusing is

$$g \cong 0.353j/r^2.$$

(3.38)

Its value is then

$$\varepsilon \cong 0.00282\varphi r\sqrt{j} \cong 0.0177nr\sqrt{j}.$$

(3.39)

Let's verify these estimations numerically. "Hook" code intended for this purpose is very similar to "Butterfly". It simulates the motion of a longitudinally uniform beam with Gaussian transverse distribution. The basic motion equation used is

$$x'' = \frac{2\widetilde{j}}{x} - gx,$$

(3.40)

where $\widetilde{j}$ is given by (3.29). Necessary mean values are always calculated as

$$<\xi> = \frac{1}{2r^2}\int\limits_0^\infty \xi y\exp\left(-y^2/2r^2\right)dy = \frac{1}{2}\int\limits_0^1 \xi\left(\frac{r\vartheta}{1-\vartheta}\right)\exp\left(-\left(\frac{\vartheta}{1-\vartheta}\right)^2\Big/2\right)\frac{\vartheta d\vartheta}{(1-\vartheta)^3},$$

(3.41)

where $y = r\vartheta/(1-\vartheta)$ is substituted to avoid infinite limits of integration.

Consider simulation results now. It was found that the minimum emittance is reached at $g = 0.38$, that is quite near the analytical estimation. The reached value in the 2π-minimum is $\varepsilon = 0.0079$ ($z = 7.15$), that is twice smaller than the analytical result ($j = 1$ and $r = 1$ every time). The results for this case are depicted in Fig. 3.5. At lower focusing, the emittance grows in both maxima and minima. For instance, at $g = 0.20$ $\varepsilon = 0.0168$ in the 2π-minimum ($z = 9.65$).
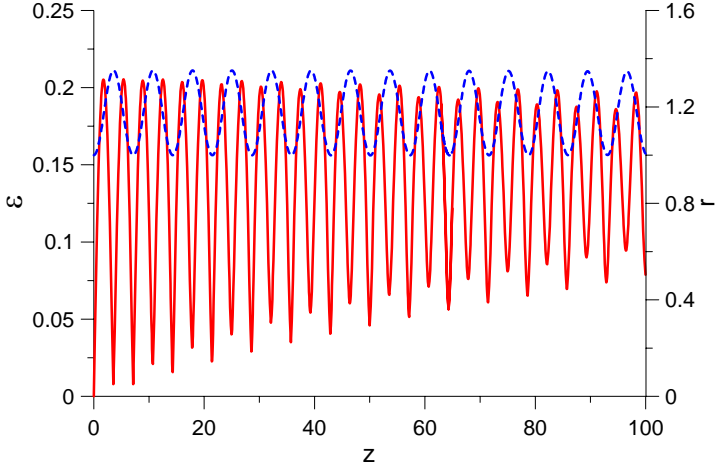
Fig. 3.5. ε (red solid) and rms-size (blue dashed) of a bunch in g = 0.38.

$g = 0.55$ is optimal for maxima Fig. 3.6. At stronger focusing, first maxima grow a little while far ones decrease.
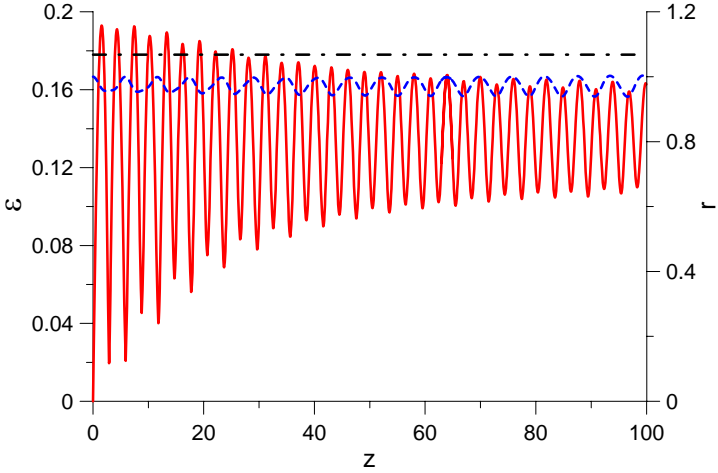
Fig. 3.6. ε (red solid) and rms-size (blue dashed) of a bunch in g = 0.55. Analytical estimate of emittance maxima (black dash-dot).

Thus the analytical estimate is improved numerically. Best emittance in $2\pi n$-minima achieved is

$$\varepsilon \cong 0.0079 nr\sqrt{j} = 0.0079 nr\sqrt{\frac{I}{I_0(\beta\gamma)^3}} \tag{3.42}$$

20

in focusing field

$$g_{2\pi} \approx 0.38 \frac{j}{r^2} \Leftrightarrow \left(\frac{eB}{2p}\right)^2 = 0.38 \frac{I}{I_0(\beta\gamma)^3} \frac{1}{r^2} .$$ (3.43)

The optimal focusing for maxima is

$$g_{max} \approx 0.55 \frac{j}{r^2} \Leftrightarrow \left(\frac{eB}{2p}\right)^2 = 0.55 \frac{I}{I_0(\beta\gamma)^3} \frac{1}{r^2} ,$$ (3.44)

and the emittance in maxima is

$$\varepsilon \approx 0.16\sqrt{jr} = 0.16\sqrt{\frac{I}{I_0(\beta\gamma)^3}}r .$$ (3.45)

The optimal focusing differs significantly for the cases of the longitudinal inhomogeneity and the transverse one, 0.09 and 0.38 respectively. Nevertheless, it should be mentioned that j means the peak current of a bunch in the first case, while the current of a stationary beam in the second one. One can estimate the "mean" current of bunch as

$$< I > = \frac{\int I^2(z)dz}{\int I(z)dz} .$$ (3.46)

This mean value is $\sqrt{2}/2$ of the peak one for a Gaussian bunch. In optimal focusing, the emittance dilution due to the longitudinal inhomogeneity is triple bigger than due to the transverse one, 0.023 vs. 0.0079.

3.3. Uniform beamline: combined effect

Consider the effect of the longitudinal inhomogeneity and the transverse one in combination. As above, assume the motion of particles independent in different slices and perfectly laminar within one slice. The beam is axially symmetric and moves in homogeneous axially symmetric linear focusing field. As the two above analytical estimates yielded not so exact results for the $2\pi n$-minimum emittance, and the dependencies of the emittance and the optimal focusing are always

$$\varepsilon \cong const \cdot nr\sqrt{j},$$

$$g_{opt} \cong const \cdot \frac{j}{r^2},$$ (3.47)

the goal is to find these constants numerically, but not focus on very complicated analytical calculations. From the two above estimates one should expect the optimal emittance value worse than in both considered cases, and the optimal focusing intermediate between above ones.

"2D" simulation code has been developed for this purpose. It is analogous to "Butterfly" and "Hook", but uses other equations. The basic motion equation for a

particle at the distance x from the axis is

$$x'' = \frac{\widetilde{I}}{I_0(\beta\gamma)^3}\frac{2}{x} - gx = \frac{2\widetilde{j}}{x} - gx,$$ (3.48)

and coincides with (3.40), but the expression for $\widetilde{j}$ differs

$$\widetilde{j} = j\exp(-\varsigma^2)\left(1 - \exp\left(-y^2/2r^2\right)\right).$$ (3.49)

Mean values for emittance evaluation are calculated as

$$<\xi> = \frac{1}{\sqrt{\pi}r^2}\int_0^\infty\int_0^\infty \xi(y,\varsigma)y\exp\left(-y^2/2r^2 - \varsigma^2\right)d\varsigma dy =$$

$$= \frac{1}{\sqrt{\pi}}\int_0^1\int_0^1 \xi(-r\ln(1-\vartheta), -\ln(1-\psi))\times$$ (3.50)

$$\times\exp\left(-\left(\frac{\vartheta}{1-\vartheta}\right)^2\bigg/2 - \left(\frac{\psi}{1-\psi}\right)^2\right)\frac{d\psi}{1-\psi}\frac{-\ln(1-\vartheta)d\vartheta}{1-\vartheta}.$$

$y = -\ln(1-\vartheta), \varsigma = -\ln(1-\psi)$ are substituted to avoid infinite integration limits. The code uses the two-dimensional Gaussian distribution of particles in a bunch. As usually, $j = 1$ and $r = 1$ every time.

It was found that the optimal focusing for 2π-emittance is $g = 0.13$. Then the emittance value is $\varepsilon = 0.037$ at $z = 11.85$ ($\varphi = \sqrt{2gz} \approx 1.92\pi$) Fig. 3.7. At lower focusing field both minima and maxima emittances increase. Focusing field $g = 0.42$ is matched to the bunch, that is oscillations of its size are minimal Fig. 3.8. Simultaneously it is optimal for maxima emittances. At stronger focusing both minima and maxima emittances increase.
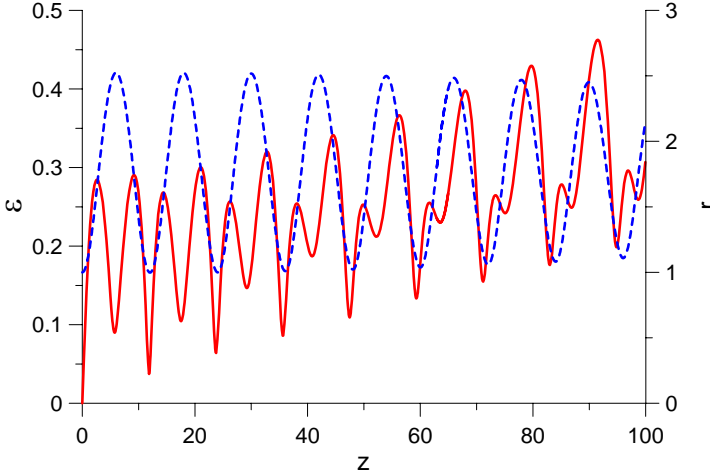
Fig. 3.7. ε (red solid) and rms-size (blue dashed) of a bunch in $g = 0.13$.
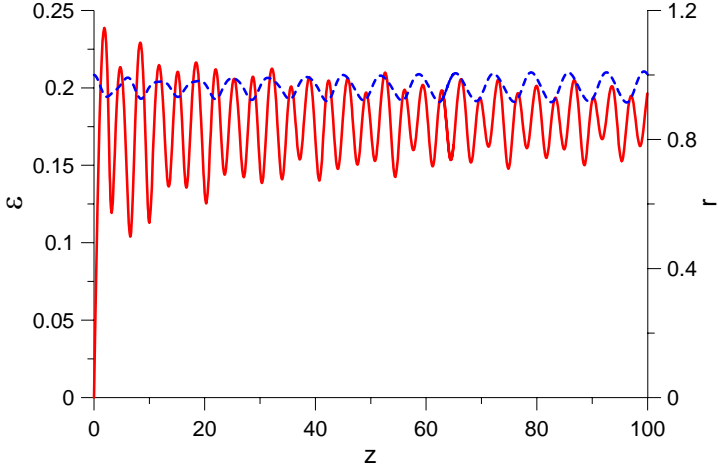
Fig. 3.8. ε (red solid) and rms-size (blue dashed) of a bunch in g = 0.42.

Thus, the optimal for minima emittances focusing in this case is

$$g_{2\pi} \approx 0.13 \frac{j}{r^2} \Leftrightarrow \left(\frac{eB}{2p}\right)^2 = 0.13 \frac{I}{I_0 (\beta\gamma)^3} \frac{1}{r^2} . \tag{3.51}$$

Then the values of emittance in the first several $2\pi n$-minima are

$$\varepsilon \cong 0.037 nr\sqrt{j} = 0.037 nr\sqrt{\frac{I}{I_0 (\beta\gamma)^3}} . \tag{3.52}$$

For emittances in maxima, the optimal focusing is

$$g_{2\pi} \approx 0.42 \frac{j}{r^2} \Leftrightarrow \left(\frac{eB}{2p}\right)^2 = 0.42 \frac{I}{I_0 (\beta\gamma)^3} \frac{1}{r^2} . \tag{3.53}$$

Then the maxima values are

$$\varepsilon \cong 0.2 r\sqrt{j} = 0.2 r\sqrt{\frac{I}{I_0 (\beta\gamma)^3}} . \tag{3.54}$$

One can see the combined effect is stronger than both above ones separately and the optimal focusing for it is intermediate between them.

3.4. Nonuniform beamline: longitudinal inhomogeneity

Uniform focusing considered in the three above sections occurs extremely rarely in real beamlines. Separate lenses are typically used to focus beams. Let's estimate the mentioned space charge effect in this case. Consider the simplest nonuniform beamline that consists of a thin solenoid and two equal empty spaces before and after it Fig. 3.9.
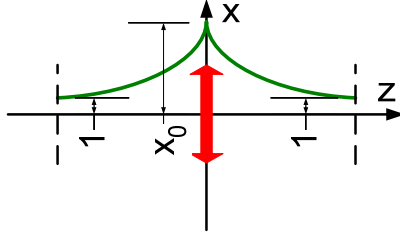
Fig. 3.9. Motion of a charged bunch in the simplest nonuniform beamline.

As in section 3.1, consider a slice with the coordinate ς in a bunch with longitudinal Gaussian distribution. The initial rms-size is 1, its derivative is 0, and the lengths and the lens strength are chosen so that the state at the exit is the same. As usually, $j = 1$. The motion equation without focusing is then

$$x'' = \frac{\exp(-\varsigma^2)}{2x}. \tag{3.55}$$

It is useful to find its analytical solution. Its Hamiltonian

$$H = \frac{p^2}{2} - \frac{\exp(-\varsigma^2)}{2} \ln x, \quad p \equiv x' \tag{3.56}$$

doesn't depend on z explicitly and, hence, is preserved. Initially $H = 0$, so one can reduce the order of the equation:

$$\frac{x'^2}{2} - \frac{\exp(-\varsigma^2)}{2} \ln x = 0 \Rightarrow x' = \sqrt{\exp(-\varsigma^2) \ln x}. \tag{3.57}$$

The explicit analytical solution of this equation is not known, but the following implicit equation can be derived:

$$z = \int_1^x \frac{d\xi}{\sqrt{\exp(-\varsigma^2) \ln \xi}}. \tag{3.58}$$

The slice is matched if $x' = 0$ at the end of the beamline for it and the neighbours. It is equivalent to the condition $x'/x = $ const at the lens. Let's find a matched beamline for a slice with the current $j_0 = \exp(-\varsigma_0^2)$. Consider a neighbour slice with the current $j_1 = j_0 + \delta j$ for this purpose. For the former slice, the half-length of the beamline z_0 is bound to the size in the lens x_0 as

$$z_0 = \frac{1}{\sqrt{j_0}} \int_1^{x_0} \frac{d\xi}{\sqrt{\ln \xi}}. \tag{3.59}$$

For the latter one

$$z_0 = \frac{1}{\sqrt{j_1}} \int_1^{x_1} \frac{d\xi}{\sqrt{\ln \xi}} = \frac{1}{\sqrt{j_1}} \left(\int_1^{x_0} \frac{d\xi}{\sqrt{\ln \xi}} + \int_{x_0}^{x_1} \frac{d\xi}{\sqrt{\ln \xi}} \right) = \frac{\sqrt{j_0}}{\sqrt{j_1}} z_0 + \frac{1}{\sqrt{j_1}} \int_{x_0}^{x_1} \frac{d\xi}{\sqrt{\ln \xi}}. \tag{3.60}$$

This expression is equivalent to the solution of the ODE:

$$\frac{dx}{dz} = \sqrt{\ln x} : x(\sqrt{j_0}\, z_0) = x_0, z \in [\sqrt{j_0}\, z_0, \sqrt{j_1}\, z_0]. \tag{3.61}$$

Assuming δj as small one can estimate x_1 using one step by the simplest second order Runge-Kutta scheme known as leapfrog:

$$x_1 = x_0 + f(x_0 + 1/2 f(x_0, z_0)\delta z, z_0 + 1/2\delta z)\delta z, \tag{3.62}$$

where $f(x,z)$ is the right part. Substituting $f(x,z)$ one obtains

$$\delta x \equiv x_1 - x_0 \cong \sqrt{\ln x_0 + 1/2\sqrt{\ln x_0}\left(\sqrt{j_1} - \sqrt{j_0}\right) z_0}\left(\sqrt{j_1} - \sqrt{j_0}\right) z_0. \tag{3.63}$$

As the Hamiltonian is preserved, the derivative immediately before the lens is

$$x_1' = \sqrt{j_1 \ln x_1}. \tag{3.64}$$

Then the condition of concordance is

$$\frac{\delta x}{x_0} = \frac{\delta x'}{x_0'} \Leftrightarrow \int_1^{x_0} \frac{d\xi}{\sqrt{\ln \xi}} = \frac{x_0 \sqrt{\ln x_0}}{\ln x_0 - 1/2}. \tag{3.65}$$

Only main terms in series expansion by δj are kept here. The only appropriate solution of this equation is $x_0 \cong 9.544162306$. In this case the integral is

$$\int_1^{x_0} \frac{d\xi}{\sqrt{\ln \xi}} \cong 8.163821003. \tag{3.66}$$

The slope immediately after the lens is

$$\tilde{x}_1' = x_1' - 2\frac{\sqrt{j_0 \ln x_0}}{x_0} x_1. \tag{3.67}$$

The Hamiltonian is

$$H = \frac{\tilde{x}_1'}{2} - \frac{j_1}{2} \ln x_1. \tag{3.68}$$

The size at the waist after the lens is

$$\tilde{\tilde{x}}_1 = \exp\left(-\frac{2}{j_1} H\right). \tag{3.69}$$

The distance from the lens to the waist is

$$z_1 = \frac{1}{\sqrt{j_1}} \int_{\tilde{x}_1}^{x_1} \frac{d\xi}{\sqrt{\ln \xi}} = \frac{\tilde{\tilde{x}}_1}{\sqrt{j_1}} \int_1^{x_1/\tilde{x}_1} \frac{d\xi}{\sqrt{\ln \xi}}. \tag{3.70}$$

It differs from z_0, so we should evaluate x_1 and x_1' out of the waist. Use the following substitution of the second order of approximation to expand the expression above by δj:

$$\int_1^{x_1/\tilde{x}_1} \frac{d\xi}{\sqrt{\ln \xi}} = \int_1^{x_0} \frac{d\xi}{\sqrt{\ln \xi}} + \int_{x_0}^{x_1/\tilde{x}_1} \frac{d\xi}{\sqrt{\ln \xi}} \cong \sqrt{j_0} z_0 + \frac{\left(x_1/\tilde{x}_1 - x_0\right)}{\sqrt{\ln\left(\left(x_0 + x_1/\tilde{x}_1\right)/2\right)}}. \tag{3.71}$$

Thus, the derivative at the end of the beamline (at z_0 from the lens) is

$$\tilde{\tilde{x}}_1' = \frac{j_1}{2\tilde{\tilde{x}}_1}\left(z_0 - z_1\right). \tag{3.72}$$

Substituting (3.59)-(3.71) and keeping only square term in expansion by δj one obtains

$$\tilde{\tilde{x}}_1' \cong -\frac{0.1654852087 \cdot \delta j^2}{j_0^{3/2}}. \tag{3.73}$$

The expressions for emittance evaluation are the same as, but one should substitute

$$x' = \tilde{\tilde{x}}_1', \ j_0 = \exp(-\varsigma_0^2), \ \delta j = \exp(-\varsigma^2) - \exp(-\varsigma_0^2). \tag{3.74}$$

The emittance reaches its minimum at $\varsigma_0 \cong 0.673$, and its value (dimensionless) is ≈ 3.32. Taking into account the current and the size one can estimate the minimal emittance as

$$\varepsilon \cong 0.0245 r \sqrt{j} = 0.0245 r \sqrt{\frac{I}{I_0 (\beta\gamma)^3}}. \tag{3.75}$$

The half-length of the beamline is then

$$z_0 \cong 10.24 \frac{r}{\sqrt{j}}, \tag{3.76}$$

while the lens strength is

$$D \cong 0.251 \frac{\sqrt{j}}{r}. \tag{3.77}$$

Let's verify this analytical estimate numerically. Code "Butterfly" has been modified for this purpose. The difference of new code "ButterflyN" is that the beam moves without focusing and a thin lens is added to the centre of the beamline. Simulation was conducted in a wide range of z_0. The results are shown in Fig. 3.10.
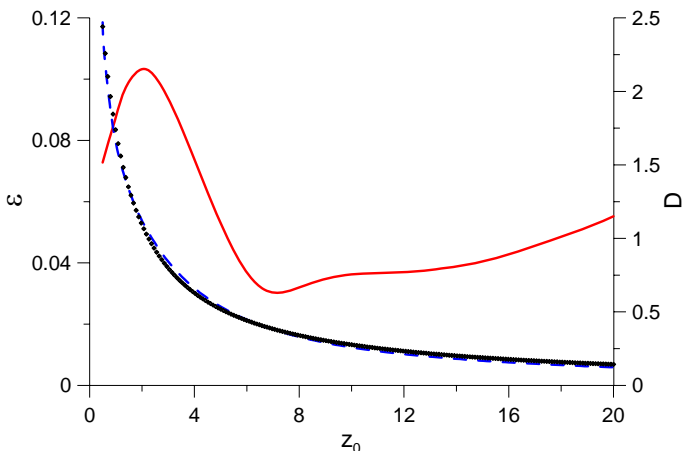
*Fig. 3.10. Minimal ε (red solid) and optimal lens strength (blue dashed)
vs. half-length of beamline.*

Obviously, the optimal beamline half-length is $z_0 \approx 7.0$. Then the emittance value is $\varepsilon \approx 0.030$ and the lens strength is $D \approx 0.381$. Note that the optimal length ($2z_0$) and the emittance value are quite near to ones in the case of uniform focusing, 14.2 и 0.023 respectively. The optimal emittance varies insignificantly in the range of half-lengths 6…15. The optimal lens strength is evaluated exactly enough by the following expression (rhombs in Fig. 3.10):

$$D = \frac{3.184}{z_0 + 0.7153}. \tag{3.78}$$

Motion through the optimal beamline is shown in Fig. 3.11.
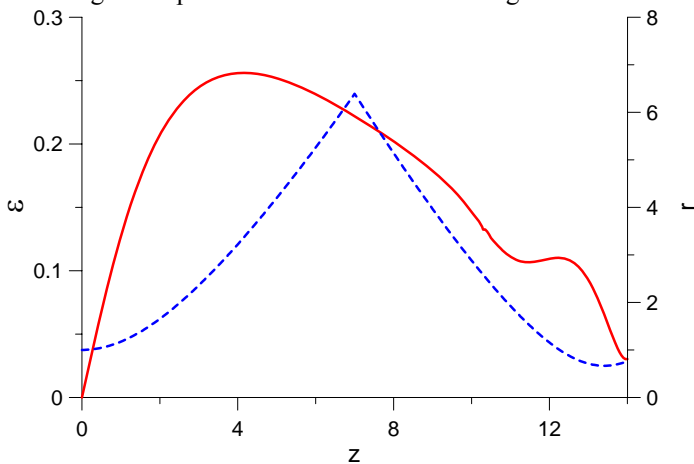
*Fig. 3.11. ε (red solid) and rms-size (blue dashed) of a bunch in a beamline with
half-length $z_0 = 7.0$ and lens strength $D = 0.381$.*

27
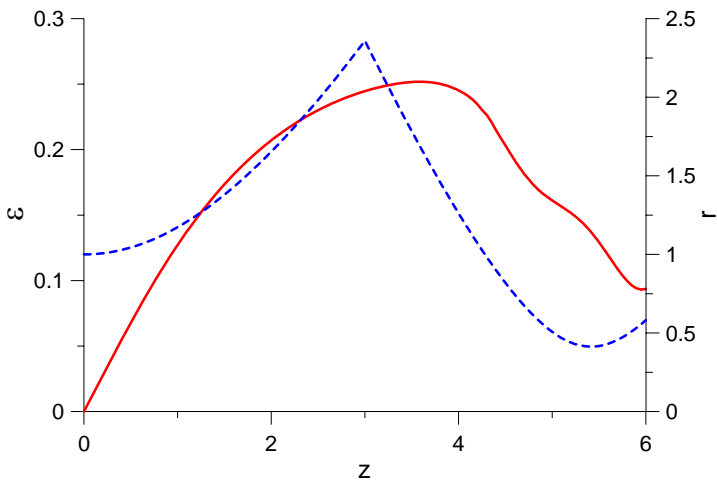
Fig. 3.12. ε (red solid) and rms-size (blue dashed) of a bunch in a beamline with half-length $z_0 = 3.0$ and lens strength $D = 0.842$.

The π-minimum here appears weakly and the bunch is overfocused, that is the end of the beamline (and the emittance minimum) is placed after the waist. At smaller z_0 the π-minimum disappears and the waist moves to the origin of the beamline Fig. 3.12. At significantly longer z_0 the π-minimum appears abruptly and shifts to the beginning of the beamline. It can even occur **before** the lens that is can be obtained in empty space with no focusing Fig. 3.13. The 2π-minimum coincides with the waist very exactly.
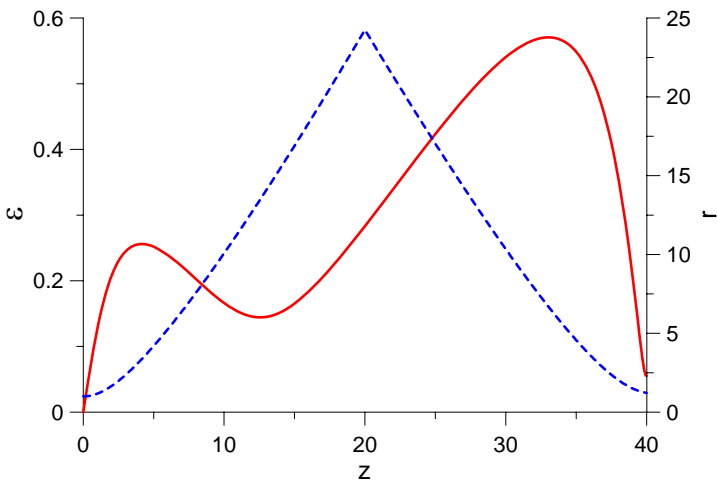
Fig. 3.13. ε (red solid) and rms-size (blue dashed) of a bunch in a beamline with half-length $z_0 = 20.0$ and lens strength $D = 0.1236$.

3.5. Nonuniform beamline: transverse inhomogeneity

To obtain similar result for the case of transverse inhomogeneity code "Hook" has been modified. The only difference of new code "HookN" is that particles move without focusing and a thin lens of the strength D is added to the middle of the beamline, at the distance z_0 from the beginning. As usually, $j = 1$ and $r = 1$ in all the cases. For each z_0, D was optimized to obtain the minimum emittance at the exit of the beamline. The results for a wide range of z_0 are depicted in Fig. 3.14. It is clear that the optimal half-length of the beamline is $z_0 \approx 4.0$. Then the emittance at the exit is $\varepsilon \approx 0.0144$ and the lens strength is $D \approx 0.688$. In contrast to the case of longitudinal inhomogeneity, the minimum of emittance is pronounced. If z_0 lies in the range 3.5…10 and the lens strength is optimal, the emittance value exceeds the global optimum not so much. The optimal lens strength can be evaluated as (rhombs in Fig. 3.14)

$$D = \frac{2.966}{z_0 + 0.7174}. \tag{3.79}$$
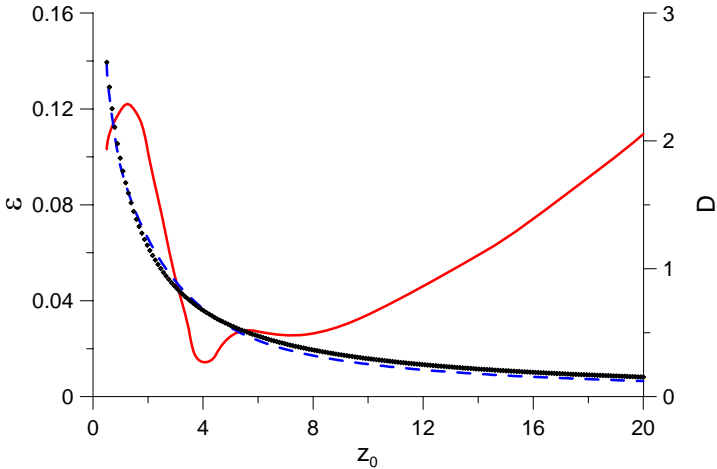
Fig. 3.14. Minimal ε (red solid) and optimal lens strength (blue dashed) vs. half-length of beamline.

Motion of a beam through the optimal beamline is shown in Fig. 3.15. The π-minimum appears abruptly, is placed not far from the 2π-one, and its value is only a little bigger. The beam is overfocused, so that the beamline exit (and the emittance minimum) is situated after the waist.
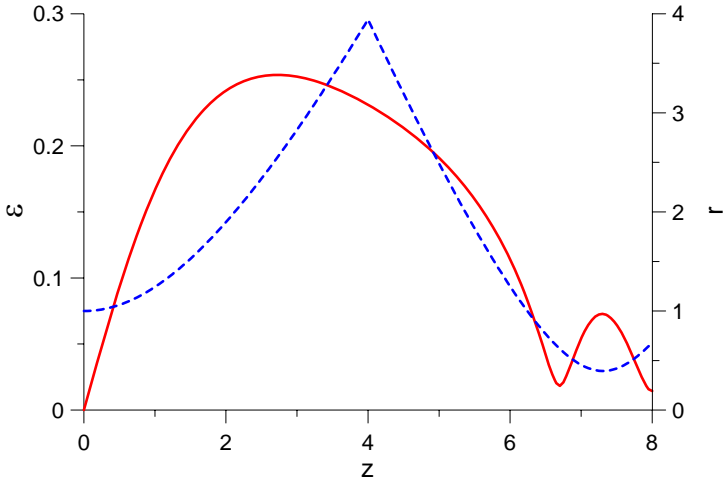
Fig. 3.15. ε (red solid) and rms-size (blue dashed) of a bunch in a beamline with half-length $z_0 = 4.0$ and lens strength $D = 0.688$.

At shorter z_0 the π-minimum disappears Fig. 3.16.
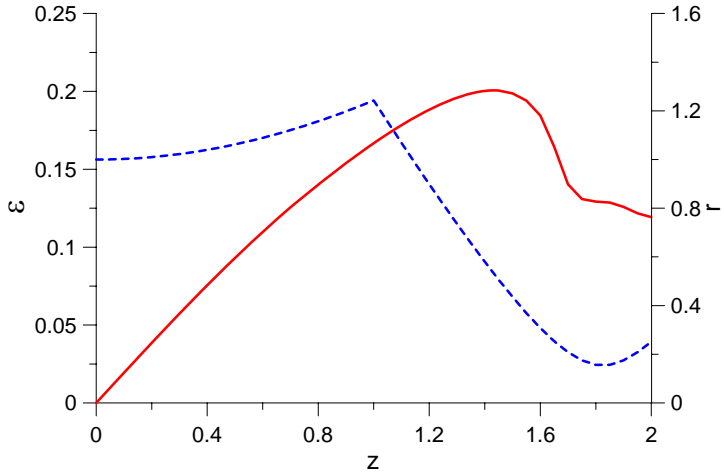
Fig. 3.16. ε (red solid) and rms-size (blue dashed) of a bunch in a beamline with half-length $z_0 = 1.0$ and lens strength $D = 1.80$.

At significantly longer z_0 the π-minimum appears clearly and is shifted to the beginning of the beamline Fig. 3.17. It can occur even before the lens that is can be obtained in empty space without focusing. The 2π-minimum coincides well with the waist. The value in the former can be smaller than in the latter.
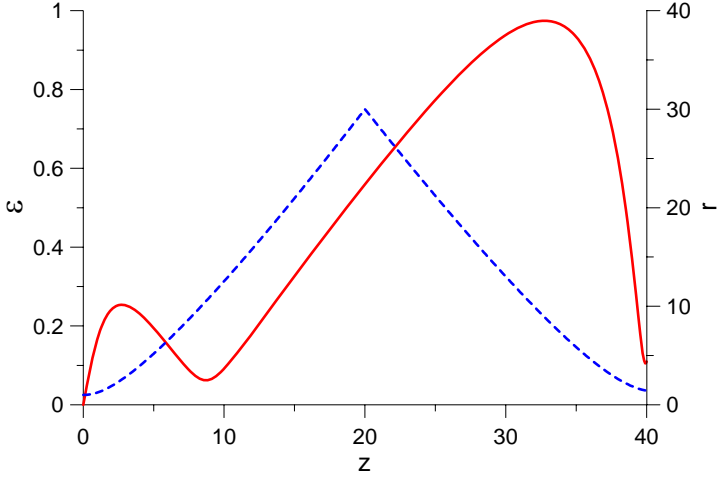
Fig. 3.17. ε (red solid) and rms-size (blue dashed) of a bunch in a beamline with half-length $z_0 = 20.0$ and lens strength $D = 0.122$.

3.6. Nonuniform beamline: combined effect

Consider the combined effect in the case of non-uniform focusing now. Code "2D" has been modified to evaluate the emittance and the parameters of the optimal beamline. The only distinction of new code "2DN" is that particles move without focusing and a thin lens of the strength D is added to the middle of the beamline, at the distance z_0 from the beginning. As usually, $j = 1$ and $r = 1$. For each given z_0, D was optimized to minimize the emittance. The results are placed in Fig. 3.18. The optimal $z_0 \approx 6.0$. It is located between the values obtained in the two sections above, and closer to the former one. Then the emittance at the exit is $\varepsilon \approx 0.0461$, and the lens strength $D \approx 0.445$. The obtained emittance value is worse than in both cases above. Note that the optimal beamline length ($2z_0$) and the emittance here are close enough to ones obtained with code "2D" for uniform focusing, 11.85 and 0.0373 respectively. If z_0 lies within 5 and 11, and the lens strength is optimal, the emittance value exceeds the optimal one not significantly. The optimal lens strength can be evaluated as follows (rhombs in Fig. 3.18)

$$D = \frac{3.118}{z_0 + 0.8080}. \tag{3.80}$$
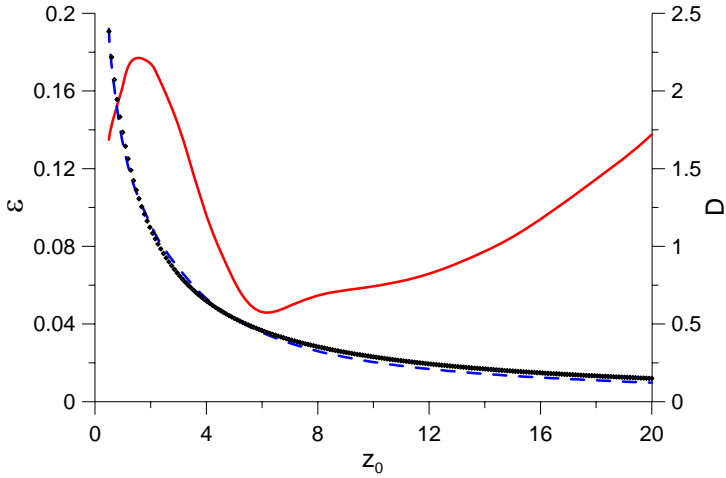
Fig. 3.18. Minimal ε (red solid) and optimal lens strength (blue dashed)
vs. half-length of beamline.

Beam motion through the optimal beamline is depicted in Fig. 3.19. The π-minimum appears weakly and the beam is overfocused that is the 2π-minimum is situated after the waist.
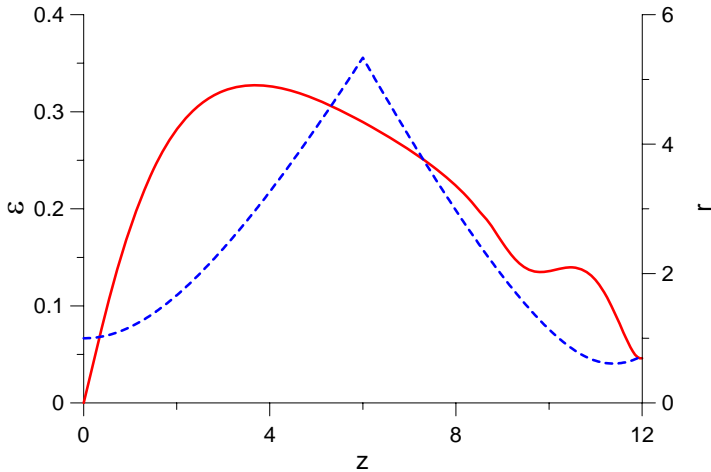
Fig. 3.19. ε (red solid) and rms-size (blue dashed) of a bunch in a beamline with
half-length $z_0 = 6.0$ and lens strength $D = 0.445$.

In shorter beamlines the π-minimum disappears and the waist moves to the entrance Fig. 3.20.
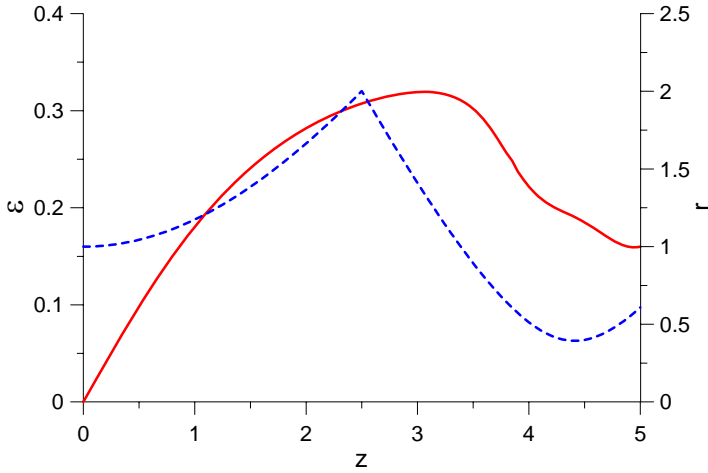
Fig. 3.20. ε (red solid) and rms-size (blue dashed) of a bunch in a beamline with half-length $z_0 = 2.5$ and lens strength $D = 0.980$.

In significantly longer beamlines π-minimum appears well and shifts to the entrance Fig. 3.21. The 2π-one exactly coincides with the waist. The values in both are comparable.
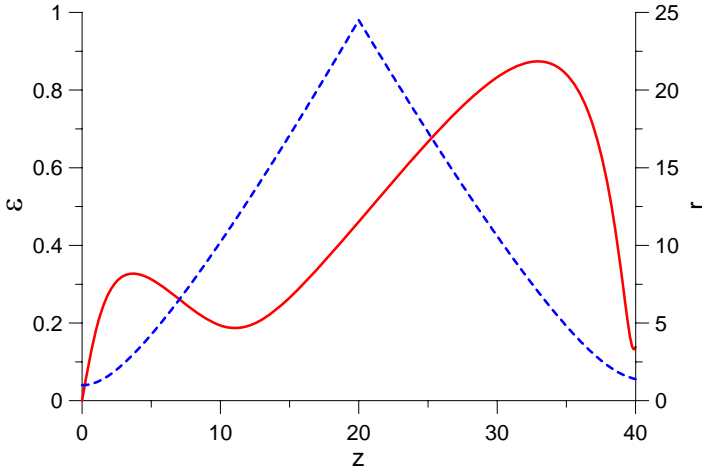
Fig. 3.21. ε (red solid) and rms-size (blue dashed) of a bunch in a beamline with half-length $z_0 = 20.0$ and lens strength $D = 0.1227$.

3.7. Matched focusing beamline with bunching

Bunching is frequently used in injectors, so taking it into account is of great interest. During bunching, j in (2.11) and $\tilde{j}$ in (2.15) are no longer constants. One still can consider a beamline where one slice (longitudinal inhomogeneity) or particle (transverse one) is always matched to the focusing. In this case the focusing in the beamline is proportional to the current. The obtained linearized equations are similar to ones used in sections 3.1 and 3.2, but their coefficients are variable. Analytical solutions of these equations in general case are not known, but one can use adiabatic approximation and so estimate the solution. The motion equation for the case of longitudinal inhomogeneity is then

$$\delta'' = -\frac{j}{x^2}\delta, \tag{3.81}$$

and its Hamiltonian is

$$H = \frac{p^2}{2} + \frac{j(z)}{2x^2}\delta^2, \, p \equiv \delta'. \tag{3.82}$$

Use the property

$$\frac{dH}{dz} = \frac{\partial H}{\partial z} \tag{3.83}$$

to estimate a solution of in adiabatic approximation. If j varies slowly enough so that $\Delta j/j << 1$ over the period of oscillation, one can approximate

$$\frac{\partial H}{\partial z} \cong \frac{j'(z)}{4x^2}a^2, \tag{3.84}$$

where a is the local relative amplitude of charge vibration. The derivative is averaged over the period. The full derivative is then

$$\frac{dH}{dz} = \frac{d}{dz}\left(\frac{\delta'^2}{2} + \frac{j(z)}{2x^2}\delta^2\right) \cong \frac{d}{dz}\left(\frac{j(z)}{4x^2}a^2 + \frac{j(z)}{4x^2}a^2\right) =$$
$$= \frac{d}{dz}\frac{j(z)}{2x^2}a^2 = aa'\frac{j(z)}{x^2} + a^2\frac{j'(z)}{2x^2}. \tag{3.85}$$

Substituting (3.84) and
(3.85) in (3.83) one can estimate the amplitude

$$aa'\frac{j(z)}{x^2} = -a^2\frac{j'(z)}{4x^2} \Rightarrow \frac{a'}{a} = -\frac{j'(z)}{4j(z)} \Rightarrow a \propto j(z)^{-1/4}. \tag{3.86}$$

It is enough to estimate emittance dilution. One should substitute the integral nonlinear phase advance

$$\Delta\varphi = \frac{1}{4}\int_0^L a^2 \cos^2\varphi(z)\frac{\sqrt{j}}{x}dz \tag{3.87}$$

in instead of (3.6). The total phase advance should be

$$\varphi = \int_0^L \frac{\sqrt{j}}{x}\,dz = 2\pi. \tag{3.88}$$

The dependencies of j and g on z are necessary to calculate both advances. Let's choose the exponential dependency

$$j \propto g \propto \exp(z/L \cdot \ln \upsilon), \tag{3.89}$$

where $\upsilon = j_1/j_0$ is the ratio of the currents at the exit and the entrance of the beamline. Then

$$\varphi = \frac{\sqrt{j_0}}{x} \int_0^L \sqrt{\exp(z/L \cdot \ln \upsilon)}\,dz = 2\frac{\sqrt{j_0}}{x}L\frac{\sqrt{\upsilon}-1}{\ln \upsilon}, \tag{3.90}$$

so

$$\Delta\varphi = \frac{a_0^2}{4} \int_0^{\frac{\pi \ln \upsilon}{\sqrt{\upsilon}-1}} \cos^2\left(\frac{2\pi\left(\exp\left(\varsigma\left(\sqrt{\upsilon}-1\right)/2\pi\right)-1\right)}{\sqrt{\upsilon}-1}\right)d\varsigma \approx \frac{\pi}{4}a_0^2 \upsilon^{-1/4}. \tag{3.91}$$

Hence

$$\varepsilon \propto r' \propto \Delta\varphi a\sqrt{j} \propto \upsilon^{-1/4}\upsilon^{-1/4}\upsilon^{1/2} = const. \tag{3.92}$$

Thus, in adiabatic approximation the compensated emittance doesn't depend on bunching. This estimation is valid only if

$$g'/g^{3/2} \ll 1, \tag{3.93}$$

that is violated frequently.

To verify this estimation, code "Butterfly" has been modified. New code "ButterflyJ" varies the current and the focusing exponentially along the beamline. Nonlinear equation (2.10) is solved, but not

(3.81). As usually, $j = 1$, $x = 1$, $x' = 0$ at the entrance. j and g increase by υ times at the exit regardless of the beamline length L. The emittance minima structure turned out to be complicated enough, so a search engine for the global minimum had to be included. The search was carried out by descent from the nodes of a logarithmically equal grid in the given area of g and L. The step of the grid was $\eta_{i+1}/\eta_i = 1.1$. The descent was performed by dual directions scheme [13] II.3. The initial focusing was limited $g < 0.5$, and the phase advance $4.5 < \varphi < 7.9$ (limits were not stiff, so the values can exceed them). The results are placed in Fig. 3.22.

The optimal beamline length decreases as $15.7/\sqrt[3]{\upsilon}$, while the optimal initial focusing fluctuates within $0.08\ldots0.11$. The emittance grows as $0.0215 \cdot \sqrt[3]{\upsilon}$. If the range of search is significantly widened, $g < 5$ и $1.5 < \varphi < 12$, the result is preserved. Evidently, it means that the 2π-minimum is global.
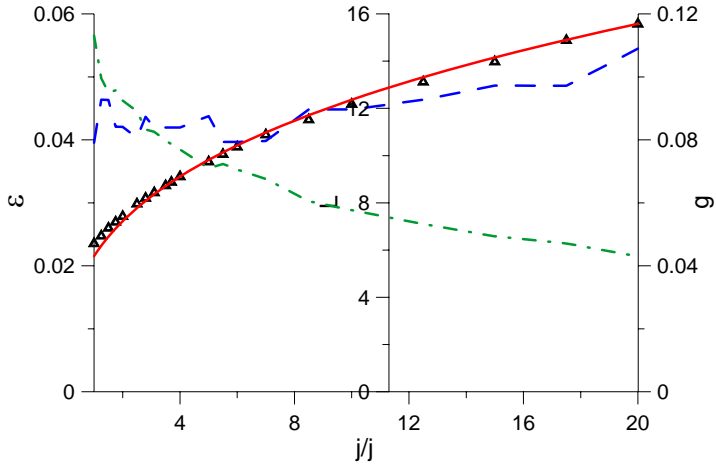
Fig. 3.22. 2π-minimal emittance (triangles; red solid is 0.0215·υ^{1/3}), and optimal focusing (blue dashed) and beamline length (green dash-dot) vs. current ratio.

A homogeneous in the longitudinal direction beam can't be bunched, so the effect of transverse inhomogeneity hardly can occur separately. Thus the only combined effect should be also considered. For numerical evaluation of the emittance, code "2D" has been modified in the same way as described for "ButterflyJ". The results obtained with new code "2DJ" are placed in Fig. 3.23. The initial focusing was limited $g < 0.5$, and the phase advance $4.5 < \varphi < 7.9$ (limits were not stiff).
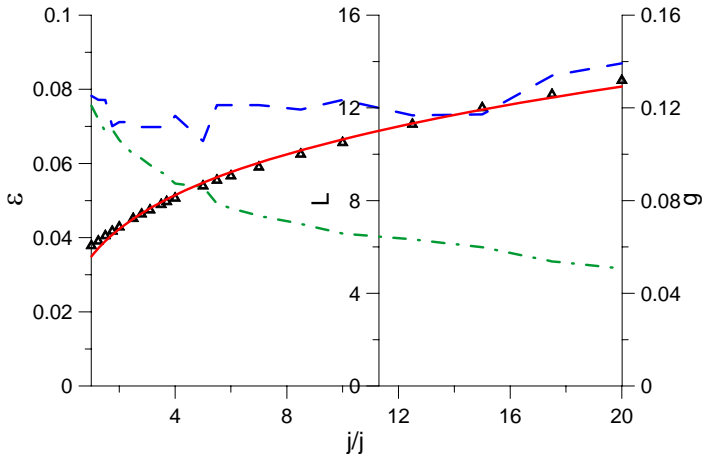
Fig. 3.23. 2π-minimal emittance (triangles; red solid is 0.0349·υ^{0.28}), and optimal focusing (blue dashed) and beamline length (green dash-dot) vs. current ratio.

The optimal beamline length decreases as $12.7 \cdot \upsilon^{-0.28}$, while the optimal initial focusing fluctuates within 0.10…0.14. The emittance increases as $0.0349 \cdot \upsilon^{0.28}$. If the range of search is significantly widened, $g < 5$ и $1.5 < \varphi < 12$, the result is preserved. Seemingly, it means that the 2π-minimum is global.

3.8. Matched focusing beamline with accelerating

An accelerating section after the buncher and/or a gun can also affect the emittance until the energy where the conditions (1.3) and (1.9) are met. To estimate the effect let's consider a beamline with matched focusing, as in 3.7. In the case of accelerating, focusing is to be proportional to $(\beta\gamma)^{-3}$. Then the equation of small vibration looks as follows

$$\delta'' + \frac{(\beta\gamma)'}{\beta\gamma}\delta' = -\frac{j}{x^2}\delta, \tag{3.94}$$

where all the coefficients are variable. In the canonical variables it is

$$\begin{cases} \delta' = \dfrac{p}{\beta\gamma}, \\ p' = -\beta\gamma\,\dfrac{j}{x^2}\delta, \end{cases} \tag{3.95}$$

where $p = \beta\gamma\delta'$. Its Hamiltonian is

$$H = \frac{p^2}{2\beta\gamma} + \frac{\beta\gamma j}{2x^2}\delta^2 = \frac{p^2}{2\beta\gamma} + \frac{I}{I_0(\beta\gamma)^2 x^2}\frac{\delta^2}{2}. \tag{3.96}$$

Use (3.83) to estimate a solution of (3.95) in adiabatic approximation. If $\beta\gamma$ varies slowly enough that is $\Delta(\beta\gamma)\,/\,(\beta\gamma) \ll 1$ during a period of vibration, one can approximate

$$\frac{\partial H}{\partial z} \cong -\frac{3}{4}(\beta\gamma)'\frac{j}{x^2}a^2. \tag{3.97}$$

The full derivative is then

$$\frac{dH}{dz} = aa'(\beta\gamma)\frac{j}{x^2} - a^2(\beta\gamma)'\frac{j}{x^2}. \tag{3.98}$$

Substituting (3.97) and (3.98) in (3.83) one can estimate the relative amplitude:

$$\frac{a'}{a} = \frac{(\beta\gamma)'}{4\beta\gamma} \Rightarrow a \propto (\beta\gamma)^{1/4}. \tag{3.99}$$

To estimate the emittance one should substitute the integral nonlinear phase advance (3.87) in (3.10) instead of (3.6). The total phase advance should be (3.88). The dependencies of $\beta\gamma$ and g on z are necessary to calculate both advances. Let's choose the exponential dependency

$$\beta\gamma \propto \exp(z/L \cdot \ln\alpha),\, g \propto \exp(-3z/L \cdot \ln\alpha), \tag{3.100}$$

where $\alpha = (\beta\gamma)_1/(\beta\gamma)_0$ is the momenta ratio at the end and the beginning of the beamline. Then the total phase advance is

$$\varphi = \frac{\sqrt{j_0}}{x} \int_0^L \left(\exp(z/L \cdot \ln\alpha)\right)^{-3/2} dz = \frac{2}{3}\frac{\sqrt{j_0}}{x}L\frac{1-\alpha^{-3/2}}{\ln\alpha}, \tag{3.101}$$

and the nonlinear part is

$$\Delta\varphi = \frac{a_0^2}{4} \int_0^{\frac{3\pi\alpha^{3/2}\ln\alpha}{\alpha^{3/2}-1}} \exp\left(\varsigma\left(\alpha^{-3/2}-1\right)/3\pi\right)\times$$
$$\times \cos^2\left(\frac{2\pi\left(\alpha^{3/2}\exp\left(\varsigma\left(\alpha^{-3/2}-1\right)/2\pi\right)-1\right)}{\left(\alpha+\sqrt{\alpha}+1\right)\left(\sqrt{\alpha}-1\right)}\right) d\varsigma \approx a_0^2\frac{\pi+\sqrt{\ln\alpha}}{4}. \tag{3.102}$$

$\Delta\varphi$ weakly depends on α (as $\approx\sqrt{\ln\alpha}$), so it can be neglected. Then the **normalized** emittance is

$$\varepsilon_n \propto r'\beta\gamma \propto \Delta\varphi a\sqrt{j}\beta\gamma \propto \alpha^{1/4}\alpha^{-3/2}\alpha = \alpha^{-1/4}. \tag{3.103}$$

The formulae above are valid only if

$$\frac{x(\beta\gamma)'}{\beta\gamma\sqrt{j}} \ll 1, \tag{3.104}$$

that is violated frequently.

To verify this estimation, code "Butterfly" has been modified. New code "ButterflyA" varies the momentum linearly along the beamline. As usually, $j = 1$, $\beta\gamma = 1$, $x = 1$, $x' = 0$ at the entrance. $\beta\gamma$, j and g were chosen as follows:

$$\beta\gamma = 1+(\alpha-1)z/L,$$
$$j = \frac{I}{I_0(\beta\gamma)^3} = \frac{j_0}{(\beta\gamma)^3}, \tag{3.105}$$
$$g = \frac{g_0}{(\beta\gamma)^3}.$$

For each slice, the following linear ODE system with variable coefficients was solved:

$$\begin{cases} x' = \dfrac{x_1}{\beta\gamma}, \\[2mm] x_1' = \beta\gamma\left(\dfrac{j}{2x} - gx\right) = \dfrac{1}{(\beta\gamma)^2}\left(\dfrac{j_0}{2x} - g_0 x\right). \end{cases} \qquad (3.106)$$

Normalized slope $x_1 \equiv \beta\gamma x'$ was used to calculate the normalized emittance. Other details are similar to code "ButterflyJ". The results for 2π-minima are shown in Fig. 3.24. The initial focusing was limited $g < 0.5$ and the phase advance

$$4.5 < \varphi = \int_0^L \sqrt{2g(z)}\,dz = \frac{2L\sqrt{2g_0}}{\sqrt{\alpha}\left(\sqrt{\alpha}+1\right)} < 7.9. \qquad (3.107)$$
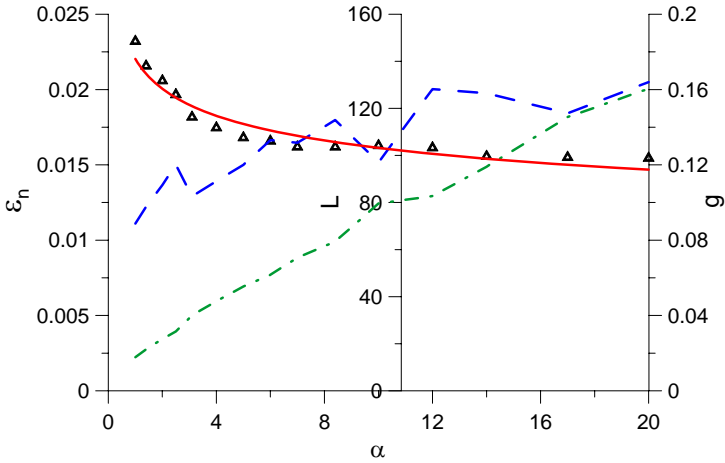
Fig. 3.24. 2π-minimal emittance (triangles; red solid is $0.0220\cdot\alpha^{-0.136}$), and optimal focusing (blue dashed) and beamline length (green dash-dot) vs. momenta ratio.

The optimal beamline length grows with α as $L \cong 11.96 + 6.05\alpha$, while the optimal initial focusing fluctuates within $0.1...0.16$. The normalized emittance diminishes as $0.0220\cdot\alpha^{-0.136}$. As in the two cases above, extension of the search area doesn't affect the results.

Consider now the combined effect in an accelerating structure. Code "2D" has been modified for this purpose the same way as described for "ButterflyA". The results of new code "2DA" at the same conditions as for "ButterflyA" are depicted in Fig. 3.25. The optimal beamline length grows with α as $L \cong 10.89 + 5.03\alpha$, while the optimal initial focusing as $g \cong 0.115\cdot\alpha^{0.227}$. The normalized emittance is varies weakly around ≈ 0.035. As in the three cases above, extension of the search area doesn't change the results.
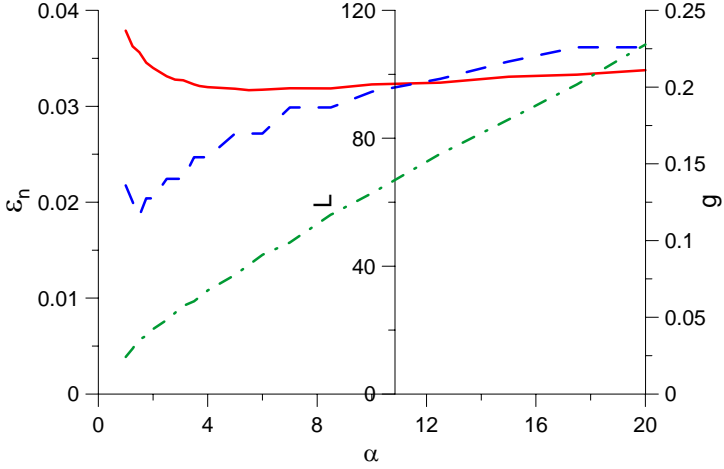
Fig. 3.25. 2π-minimal emittance (red solid), and optimal focusing (blue dashed) and beamline length (green dash-dot) vs. momenta ratio.

3.9. Summary

For the convenience, the formulae for beamlines obtained in Sections 3.1 - 3.8 are collected here. The appropriate coefficients are accumulated in Table 3.1. The 2π-minimal normalized emittance at the end of an optimal beamline can be estimated as

$$\varepsilon_n \cong \varepsilon^c r \sqrt{\frac{|I|}{I_0 \beta \gamma}}. \tag{3.108}$$

The length of the optimal beamline is

$$L \cong L^c r \Big/ \sqrt{\frac{|I|}{I_0 (\beta\gamma)^3}}. \tag{3.109}$$

The distributed focusing gradient in a matched beamline is

$$g \cong \frac{g^c}{r^2} \frac{|I|}{I_0 (\beta\gamma)^3}. \tag{3.110}$$

The lens strength in a simplest non-uniform beamline is

$$D \cong \frac{D^c}{r} \sqrt{\frac{|I|}{I_0 (\beta\gamma)^3}}. \tag{3.111}$$

If the energy or the peak current is variable, all the parameters belong to the beginning of a beamline. The listed formulae and coefficients can be also used to estimate the initial approximation for precise simulation and optimization of a beamline.

Table 3.1. Parameters of optimal beamlines.

Parameter	Uniform beamline		
	Longitudinal	Transverse	Combined
ε^c	0.023	0.0079	0.037
g^c	0.09	0.38	0.13
L^c	14.2	7.15	11.85
	Nonuniform beamline		
ε^c	0.030	0.0144	0.0461
D^c	0.381	0.688	0.445
L^c	14.0	8.0	12.0
	Distributed focusing : bunching		
ε^c	$0.0215 \cdot \sqrt[3]{\upsilon}$		$0.0349 \cdot \upsilon^{0.28}$
g^c	0.08…0.11		0.10…0.14
L^c	$15.7 / \sqrt[3]{\upsilon}$		$12.7 \cdot \upsilon^{-0.28}$
	Distributed focusing : accelerating		
ε^c	$0.0220 \cdot \alpha^{-0.136}$		0.035
g^c	0.1…0.16		$0.115 \cdot \alpha^{0.227}$
L^c	$11.96 + 6.05\alpha$		$10.89 + 5.03\alpha$

4. Electron guns

4.1. Effect of longitudinal inhomogeneity in guns

A source of electrons (also protons or ions) always emits particles with quite low energy. Thus j and hence the space charge effect are strongest in this area. Unfortunately, the model described above doesn't work in this area due to the following reasons:

1. Conducting electrodes ever occur nearby an emitter. Their charge distributions depend on the one in the beam and produces fields comparable to the ones of the beam charge. Thus the effect of electrodes is defining near an emitter.

2. If a beam is transient (consists of bunches), then an area always exists where its energy is low enough and the bunch length in the moving frame is comparable or smaller than its transverse sizes. In this case coupling between different slices is significant.

3. The head and the tail of a bunch move in different conditions: when the head is being born, the bunch is absent, while when the tail is being born, the bunch has been already emitted. Moreover, during acceleration, a lower energy bunch is situated behind the head, while a higher energy one passes ahead of the tail. The transverse forces are different in this case due to non-locality of interaction. Hence the gained transverse momentum depends not only on the local current, but also on the longitudinal coordinate in a bunch.

If the emitter is circular and the beam is stationary, the gun geometry can be optimized so that space charge effect doesn't cause emittance dilution. Well-known Pierce gun [14] is an example. At the same time longitudinal inhomogeneity ever corrupts the emittance as a gun can be optimal for a given current only, and the phase portraits of slices with different currents are distorted and rotated with respect to the optimal one.

The trajectories of particles in a gun preserve if its voltage and current meet Child-Langmuir law $I \propto U^{3/2}$ (only if nonrelativistic). In this case the emittance (not normalized!) doesn't depend on the current. The quality factor of a gun is $\varepsilon / (r\sqrt{j})$. Let's determine its dependency on the voltage and the current in the nonrelativistic case.

$$\beta\gamma \cong \sqrt{2eU/mc^2} \propto \sqrt{U} \Rightarrow j = \frac{I}{I_0(\beta\gamma)^3} \propto \frac{U^{3/2}}{U^{3/2}} = const, \tag{4.1}$$

that is it depends only on the geometry (ε and $r = $ const). At the same time, the brightness is $I/\varepsilon_n^2 \propto \sqrt{U}$. If all the sizes are varied proportionally and the current density from the emitter is preserved, $\varepsilon \propto r, I \propto r^2, U \propto r^{4/3}$, so the quality factor is

$$\frac{\varepsilon}{r\sqrt{j}} \propto \frac{r(\beta\gamma)^{3/2}}{r\sqrt{I}} \propto \frac{U^{3/4}}{r} = const. \tag{4.2}$$

The brightness in this case is proportional to $\sqrt{U}/r^2$, but the increase of the voltage and the current density is restricted by the electric strength and the emissive ability.

As the basic scaling is derived, one should only determine the coefficient at $r\sqrt{j}$ in the expression for the emittance and the optimal ratio of the gun length to the emitter radius. Another important parameter is the charge phase at the gun exit as the further beamline should add a $2\pi n$'s complement to minimize the final emittance.

SAM [15], a 2D steady-state code, was used to simulate guns. The phase portraits of the beam at the exit were calculated for a set of homogeneously emitted currents. Each result was considered as the state of the slice with the given

current. A diode gun similar to used in [16] has been simulated first Fig. 4.1. The emitter radius was 5 mm, the distance between the electrodes was 123 mm, while the beam was observed at 200 mm from the cathode. The optimal current was 2 A at 300 kV that corresponds well to the "natural" perveance.
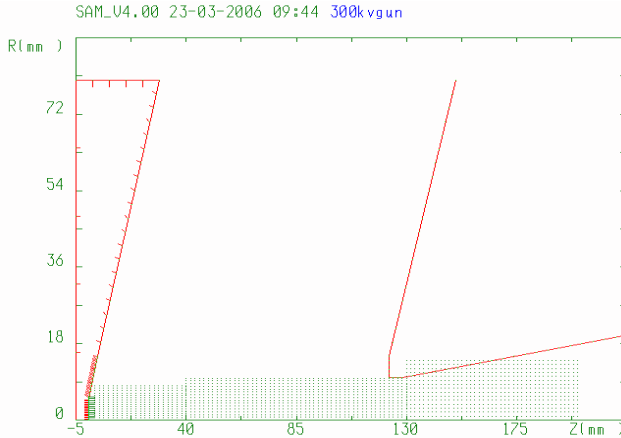
Fig. 4.1. The geometry of the basic gun, red solid lines are electrodes.

The calculated beam parameters depending on the beam current are depicted in Fig. 4.2. They were calculated by the following formulae:

$$x = \sqrt{<x^2>},$$

$$x' = <xx'> / \sqrt{<x^2>}, \tag{4.3}$$

$$\varepsilon = \sqrt{<x^2><x'^2> - <xx'>^2}.$$
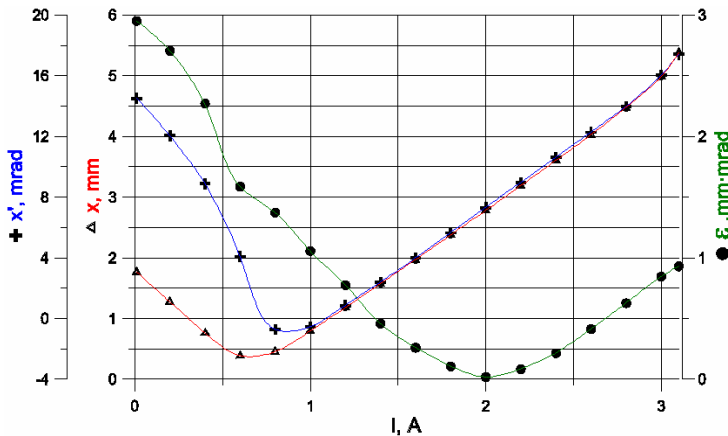
Fig. 4.2. Beam parameters vs. beam current: rms-size,
its derivative and emittance.

43

Let's calculate the charge phase and the relative charge amplitude from these data now. The beam size at the cathode preserves, but its **homothetic** size $x \propto \sqrt{I}$ (section 2.1), so that

$$\frac{\partial x}{\partial I} = \frac{1}{2}\frac{x}{I}. \tag{4.4}$$

Than the initial charge vibration amplitude is

$$\delta x = -\delta I \frac{\partial x}{\partial I} = -\frac{1}{2}x\frac{\delta I}{I} \quad \Rightarrow \quad \frac{\partial \delta_0}{\partial I} = -\frac{1}{2I}. \tag{4.5}$$

The dimensionless deviation from the **homothetic** trajectory at the gun exit is

$$\delta = \frac{\delta x - \dfrac{1}{2}x\dfrac{\delta I}{I}}{x} = \left(\frac{1}{x}\frac{\partial x}{\partial I} - \frac{1}{2I}\right)\delta I \quad \Rightarrow \quad \frac{\partial \delta}{\partial I} = \frac{1}{x}\frac{\partial x}{\partial I} - \frac{1}{2I}, \tag{4.6}$$

and its derivative by the longitudinal coordinate is

$$\delta' \equiv \left(\frac{\delta x}{x}\right)' = \frac{\delta x'}{x} - x'\frac{\delta x}{x^2} \quad \Rightarrow \quad \frac{\partial \delta'}{\partial I} = \frac{1}{x}\frac{\partial x'}{\partial I} - \frac{x'}{x^2}\frac{\partial x}{\partial I}. \tag{4.7}$$

As $\partial\delta_0/\partial I$ is negative at the emitter, the significant matrix elements are

$$C \propto \frac{\partial \delta}{\partial I}, C' \propto \frac{\partial \delta'}{\partial I}, \tag{4.8}$$

and the charge phase at the gun exit is

$$\varphi = \arctan\left(\frac{-C'x}{C\sqrt{j}}\right) = \arctan\left(\frac{\dfrac{\partial x'}{\partial I} - \dfrac{x'}{x}\dfrac{\partial x}{\partial I}}{\left(\dfrac{1}{2I} - \dfrac{1}{x}\dfrac{\partial x}{\partial I}\right)\sqrt{j}}\right). \tag{4.9}$$

The quadrant should be selected so as the signs of $\sin\varphi$ and $\cos\varphi$ coincide to the ones of the numerator and the denominator respectively.

To calculate the relative charge amplitude one should compare $\partial\delta/\partial I$ with the same derivative for a beam starting at the same point with fixed initial conditions, that is $\partial\delta/\partial I = -1/2I$, and $\partial\delta'/\partial I$ with the latter multiplied by the local wavenumber, that is $\partial\delta'/\partial I = -1/2I \cdot \sqrt{j}/x$. The root of the sum of the squares of these ratios gives the relative amplitude:

$$A = \sqrt{\left(\frac{2I}{x}\frac{\partial x}{\partial I} - 1\right)^2 + j\left(2I\left(\frac{\partial x'}{\partial I} - \frac{x'}{x}\frac{\partial x}{\partial I}\right)\right)^2}. \tag{4.10}$$

The dependencies of the phase and the amplitude on the current for the mentioned gun are shown in Fig. 4.3.
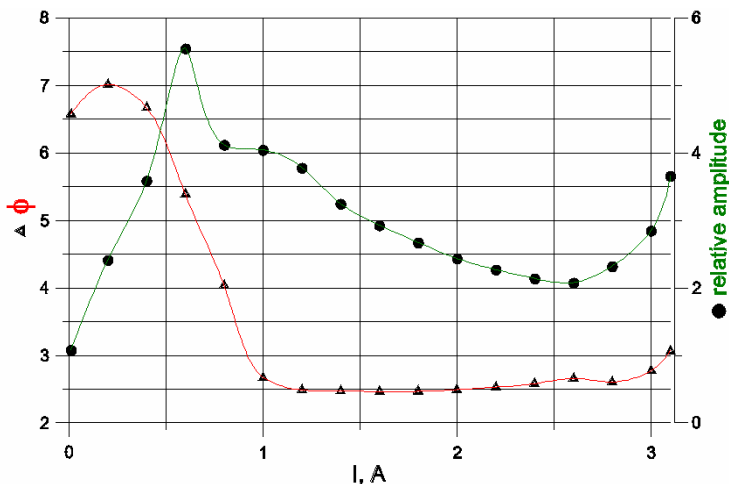
Fig. 4.3. Charge phase and relative amplitude vs. beam current.

It is seen that the phase is almost constant within current limits from 1 to 3 A and its value is $\approx 2.5 \approx 0.8\pi$. Thus, if an ideal uniform beamline (where the phase advance doesn't depend on the amplitude) with the phase advance $\approx 1.2\pi$ is placed after the gun, one should expect the minimal emittance. The following questions are still left: (i) what peak current of a bunch gives the minimum emittance in this system, (ii) which slice should be matched to the compensation beamline, and (iii) what is the optimal phase advance of the latter. The dependency of the compensated emittance of a 2.2 A (peak current) Gaussian bunch on the matched slice current and the charge phase is placed in Fig. 4.4. An ideal compensation
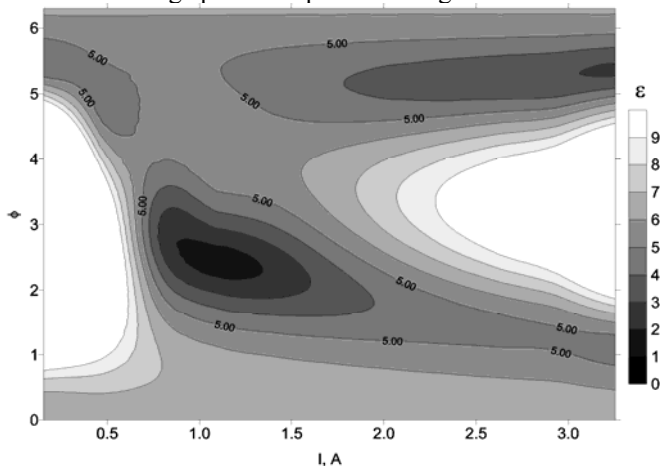
Fig. 4.4. Compensated emittance of Gaussian bunch of 2.2 A peak current vs. charge phase and matched current.

beamline (equation (2.11)) with the phase advance $2\pi - \varphi$ and matched with the given current was added after the gun. The global minimum 1.52 mm·mrad is reached at the matched current 1.144 A and the phase advance $2\pi - 2.49 \cong 1.207\pi$ in the compensation beamline. Without the beamline, the emittance due to phase portraits fanning (pure longitudinal inhomogeneity effect) is 6.14 and the full one (combined effect) 6.89 mm·mrad at the same peak current. The dependencies of the emittance and the quality factor $\varepsilon/\sqrt{j}$ (all the sizes are preserved) on the peak current without compensation are shown in Fig. 4.5. Upper curves include slice emittances. The non-compensated emittance is proportional to the peak current in both cases if $I_{\rm p} > 0.7$ A. Hence $\varepsilon/\sqrt{j} \propto \sqrt{I}$.
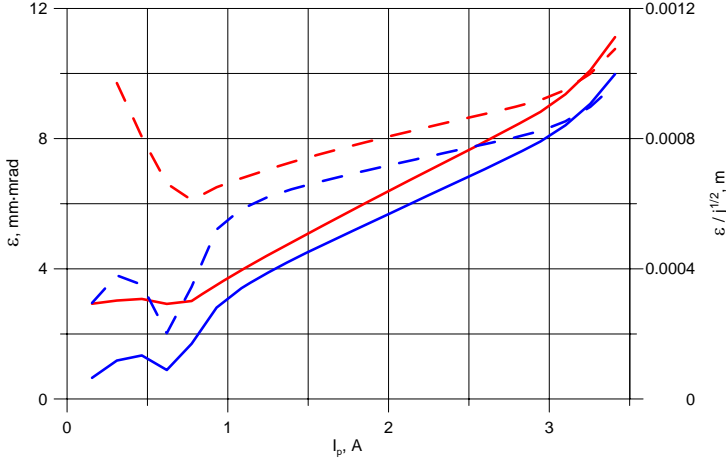
Fig. 4.5. Non-compensated emittance of Gaussian bunch (solid) and $\varepsilon/\sqrt{j}$
(dashed) vs. peak current. Upper (red) curves include slice emittance.

Similar compensated values one can find in Fig. 4.6. The phase advance and the matched current of an ideal compensation beamline were optimized for each given peak current. The addition due to the slice emittances was calculated as

$$\varepsilon_4 = \sqrt{\varepsilon_3^2 + \varepsilon_2^2 - \varepsilon_1^2}, \qquad (4.11)$$

where ε_1 and ε_2 are the lower curve and the upper one in Fig. 4.5 while ε_3 and ε_4 are the same in Fig. 4.6. In other words, the differences of squares of the curves in Fig. 4.5 and Fig. 4.6 are equal. The matter is that some slices have a crossover at the end of the beamline, so the calculated rms derivative

$$<x'^2> = \frac{\varepsilon^2 + <xx'>^2}{<x>^2} \qquad (4.12)$$

is unrestrictedly large. Thus, a more proper method is hardly possible in this model.
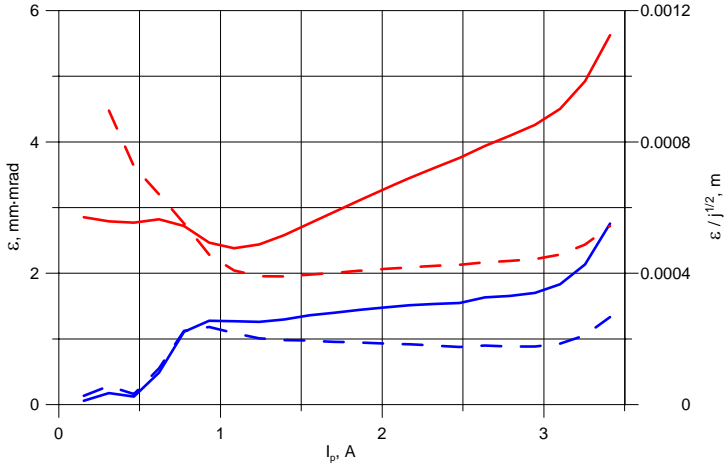
Fig. 4.6. Compensated emittance of Gaussian bunch (solid) and $\varepsilon/\sqrt{j}$ (dashed) vs. peak current. Upper (red) curves include slice emittance.

$\varepsilon/\sqrt{j}$ in this case almost doesn't depend on the peak current in the range 1...3 A and amounts to $\approx 2 \cdot 10^{-4}$ m without slice emittances and $\approx 4 \cdot 10^{-4}$ m with them. As the rms size at the emitter is $x = r/2 = 2.5$ mm, the quality factor is ≈ 0.08 and ≈ 0.16 respectively. The effect of the imperfection of the compensation beamline can be estimated as ((3.6), (3.13), (3.108), Fig. 3.3 and Table 3.1)

$$0.023 \frac{x_1}{x} a^3 \frac{\varphi}{2\pi} \approx 0.27, \tag{4.13}$$

where x_1 is the size of the matched slice at the gun exit, a is the relative amplitude of charge vibration Fig. 4.3, and φ is the phase advance in the beamline. In this case the beamline contains a thin lens (as typically $x' > 0$ for the matched slice at the gun exit) and uniform focusing further. So the effect of longitudinal inhomogeneity in the gun is about the same in a uniform beamline with the same amplitude and phase advance. The combined effect is approximately twice stronger that also corresponds to a uniform beamline.

Four other guns have been simulated in the same way to investigate the influence of the gun geometry. The emitter radius was equal while the length was varied. The electrodes were shaped to make perfect electric field. Additional electrodes were added to the guns "Short 2" and "Long 2" to equalize their perveance to the primary one. The optimal current in all the cases was ≈ 2 A. The plots for these guns are similar to Fig. 4.2 - Fig. 4.6 and were omitted here. The results for all the simulated guns are placed in Table 4.1. The observation point position is measured from the cathode. The last column considers the slice emittances. All the calculated values are valid for the range of peak current 1...3 A.

Table 4.1. Simulated gun parameters.

Gun	Length, mm	Observation point, mm	U, kV	φ	$\varepsilon/\sqrt{j}$, m	$\varepsilon/\sqrt{j}$ (slices), m
Basic	123	200	300	2.5	$2 \cdot 10^{-4}$	$4 \cdot 10^{-4}$
Short	61.5	100	150	2.2	$7.5 \cdot 10^{-5}$	$4.8 \cdot 10^{-4}$
Short 2	61.5	100	300	2	$2.5 \cdot 10^{-4}$	$5 \cdot 10^{-4}$
Long	246	400	850	2.5	$4 \cdot 10^{-4}$	$5.4 \cdot 10^{-4}$
Long 2	246	400	300	3.1	$1.2 \cdot 10^{-4}$	$4.6 \cdot 10^{-4}$

It should be mentioned that the charge phase at the gun exit varies from 2 to 3.1 only while the gun length is quadrupled. Note that the observation point is ever placed beyond the electric field area and a beam moves through some empty space proportional to the gun length. $\varepsilon/\sqrt{j}$ ratios with slice emittances of all the considered guns are almost equal, $\varepsilon/\sqrt{j} = (4.7 \pm 0.7) \cdot 10^{-4}\,\text{m}$.

Thus, emittance compensation applied to an electron gun always improves emittance several times. The expected compensated normalized emittance of a well-designed gun with an ideal compensation beamline is

$$\varepsilon_n \approx 0.2 x_e \sqrt{\frac{I}{I_0 \beta \gamma}} = 0.1 r_e \sqrt{\frac{I}{I_0 \beta \gamma}}, \tag{4.14}$$

where r_e is the emitter radius and x_e is the rms beam size at the emitter. A non-ideal optimal compensation beamline worsens this value to

$$\varepsilon_n \approx 0.45 x_e \sqrt{\frac{I}{I_0 \beta \gamma}} = 0.225 r_e \sqrt{\frac{I}{I_0 \beta \gamma}}. \tag{4.15}$$

The charge phase advance of the compensation beamline should be $1.05\ldots1.35\pi$. The compensation beamline should be matched to the $0.5\ldots0.75$ of the peak current.

4.2. Grid effects

At least three grid effects should be taken into account:
1. Scattering on the cells (not connected to space charge directly).
2. Focusing in cells at non-optimal current.
3. Space charge inhomogeneity owing to thinning out.

Let's estimate scattering first Fig. 4.7.
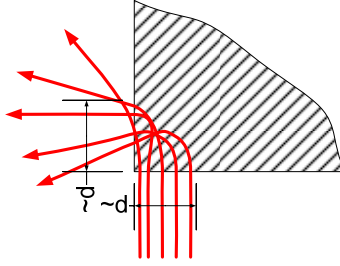
Fig. 4.7. Scattering on grid.

If U is the cathode-to-grid voltage, then the normalized transverse momentum of scattered electrons is

$$\frac{p}{mc} < \sqrt{2\frac{eU}{mc^2}}, \tag{4.16}$$

and the portion of the scattered electrons is

$$\frac{\Delta N}{N} < \frac{d}{4l} < \frac{U}{4W\rho l}, \tag{4.17}$$

where $W \approx W_0/\beta^2 \approx W_0 \cdot mc^2/2eU$ is the ionization loss (see [17], Bethe formula (1.16) and Table 1.6), $W_0 \approx 2$ MeV/g·cm$^2 = 2\cdot10^5$ eV/kg·m^2; and l is the ratio of the area of a cell to its perimeter. Flammersfield formula [18], (25b) yields a little smaller penetration depth. It is taken into account that (i) not more than a half of electrons fly out the left edge (Fig. 4.7) and (ii) not more of the latter have the momentum directed upwards, all the others can't move beyond the grid. Then the added normalized emittance can be calculated as

$$\varepsilon_n = \frac{pc}{mc^2}r\sqrt{\frac{\Delta N}{N}} < r\frac{eU}{mc^2}\sqrt{\frac{U}{W_0\rho l}}. \tag{4.18}$$

For example, for cathode-grid unit Y-824 made by CPI/Eimac (the cathode diameter 16 mm, the cathode-to-grid distance 0.2 mm, the size of a square cell 0.55 mm) this value is $\approx 2.9\cdot10^{-8}$ m at the cathode-to-grid voltage 100 V. Apparently, this effect doesn't contribute to the total emittance, but generate a very small amount of electrons with large transverse momentum.

Let's estimate the emittance on account of focusing in cells of a grid. In a round cell (also not a bad approximation for a square one), the flux incoming to the grid is

$$\Delta\Phi = \pi R^2 \Delta E = 2\pi R \int E_R dz \Rightarrow \int E_R dz = \frac{\Delta ER}{2}, \tag{4.19}$$

where R is the cell radius, ΔE is the field difference on the grid surfaces, and E_R is the radial field. The gained transverse momentum of a particle is

$$p = \frac{e}{v} \int E_R dz, \qquad (4.20)$$

and the normalized tilt at the cell edge is

$$X_n' = \frac{p}{mc} = \frac{e}{mcv} \int E_R dz = \frac{\Delta ER}{2\sqrt{2U\,mc^2/e}}. \qquad (4.21)$$

Thus the gained emittance is

$$\varepsilon_n = \sqrt{<x^2><x_n'^2>} = \frac{r \cdot \Delta ER}{8\sqrt{2U\,mc^2/e}}, \qquad (4.22)$$

where r is the emitter radius. Properties $<x^2> = r^2/4$ and $<x_n'^2> = X_n'^2/4$ were used.

For slit-like cells Fig. 4.8 that often occur in grids the appropriate formulae are:

$$\Delta\Phi = d\Delta E = 2\int E_x dz \Rightarrow \int E_x dz = \frac{\Delta Ed}{2}, \qquad (4.23)$$

$$X_n' = \frac{p}{mc} = \frac{e}{mcv} \int E_x dz = \frac{\Delta Ed}{2\sqrt{2U\,mc^2/e}}, \qquad (4.24)$$

$$\varepsilon_n = \sqrt{<x^2><x_n'^2>} = \frac{r \cdot \Delta Ed}{8\sqrt{2U\,mc^2/e}}. \qquad (4.25)$$

$<x_n'^2> = X_n'^2/2$ for a slit, but only a half of cells focus in the selected direction.
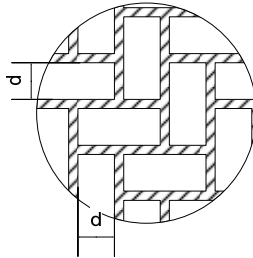
Fig. 4.8. Slit-like cells grid.

The field between the grid and the cathode is

$$I \propto U^{3/2} \Rightarrow E \propto I^{2/3}. \qquad (4.26)$$

The field outside the grid depends also on the gun geometry. Consider the basic gun from Section 4.1 and assume that the matched current ($\Delta E = 0$) coincides with the optimal one. Then one can calculate the field at the grid and plot the dependency of ΔE on I Fig. 4.9: $d\Delta E/dI \approx -0.467\,\text{MV/(m·A)}$ with good accuracy.

Then the normalized emittance depending on the peak current of a Gaussian bunch can be calculated (a grid of mentioned Y-824 was taken) Fig. 4.10.
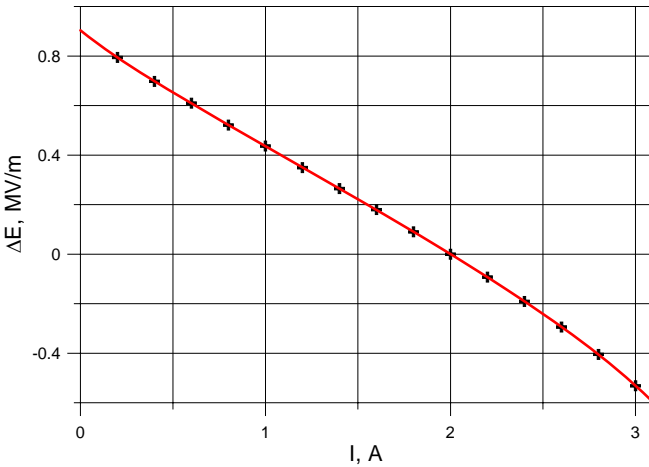
Fig. 4.9. Field step across grid vs. current.
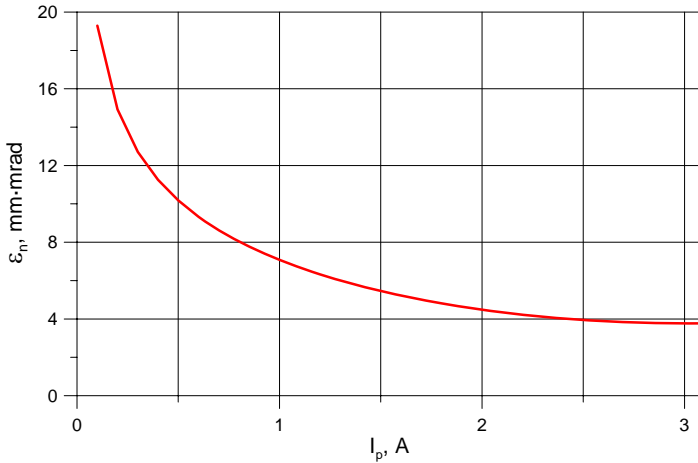
Fig. 4.10. Normalized emittance vs. peak current.

The compensated emittance of the same gun grows as square root of the peak current in the range 1…3 A (Fig. 4.6) and is $\varepsilon \approx 3.3 \rightarrow \varepsilon_n \approx 4.1$ mm·mrad at 2 A. Thus, at peak current exceeding 2 A the grid emittance is smaller than the space charge one. The results for other considered guns are very close to this.

Now it would be very useful to find a scaling formula for grid emittance. Independent variables are: the emitter radius r, the peak current I, the cell size d, and the cathode-to-grid distance D. U depends on these parameters as

$$U \propto \left(\frac{I}{r^2}\right)^{2/3} D^{4/3}. \tag{4.27}$$

The field on the grid on the cathode side is

$$E_1 \propto \left(\frac{I}{r^2}\right)^{2/3} D^{1/3}, \tag{4.28}$$

while on the other side

$$E_2 \propto \left(\frac{I}{r^2}\right)^{2/3}. \tag{4.29}$$

On the assumption that the effect of E_1 is dominant, the emittance is

$$\varepsilon_n \propto d\left(\frac{rI}{D^2}\right)^{1/3}. \tag{4.30}$$

If, on the contrary, the outside field E_2 determines ΔE, then

$$\varepsilon_n \propto d\left(\frac{rI}{D}\right)^{1/3}. \tag{4.31}$$

As the effects of both fields are comparable, the truth lies in the middle:

$$\varepsilon_n \approx 0.01 \frac{(rI)^{1/3} d}{\sqrt{D}}. \tag{4.32}$$

Coefficient 0.01 is dimensional, so one should take the values in meters and Amperes.

Owing to thinning out a beam by the grid, the current density becomes inhomogeneous Fig. 4.11. The effect can be considered as in Sections 2.2 and 3.2. Assuming the motion of a slice as the principal trajectory, one can treat the motion of an area with current as its disturbance.
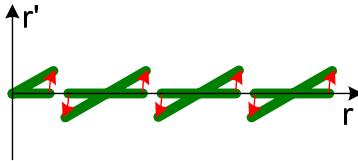
Fig. 4.11. Thinning out beam by grid.

In contrast to Fig. 4.11, the real phenomenon is 2D and the current areas are not concentric circles. After a slit-like grid, the motion approximates to 1D. The areas move independently until their edges do not cross. After that, the disturbing transverse force oscillates around zero for a given particle and the mean disturbed momentum of the latter preserves. It is owing to crossing of more and more edges of primary current areas. If the cells are square, crossing of the edges occur not

52

simultaneously over the perimeter, but the basic phenomenon remains. Thus, the emittance is effected by:

1. The beam size x.
2. The local wavenumber of charge vibration $\sqrt{j}/x$.
3. The relative amplitude of charge vibration A.
4. The cell size χ.
5. The transparency of the grid v.

$$\varepsilon \approx xx' \approx x \cdot \chi A\left(1 - \sqrt{v}\right)\frac{\sqrt{j}}{x} \approx \frac{1}{2}\chi A(1-v)\sqrt{j}. \qquad (4.33)$$

As usually, rms values are presumed: one should take $\chi = d/4$ for square cells and $\chi = d/2\sqrt{2}$ for slit0like ones, where d is the period of a square cells grid and the slit width for a slit-like one. In the latter case, only a half of cells contribute to x', so the result should be divided by $\sqrt{2}$. So the result is

$$\varepsilon \approx \frac{1}{8}Ad(1-v)\sqrt{j} = \frac{1}{8}Ad(1-v)\sqrt{\frac{I}{I_0(\beta\gamma)^3}} \Rightarrow \varepsilon_n \approx \frac{1}{8}Ad(1-v)\sqrt{\frac{I}{I_0\beta\gamma}}. \qquad (4.34)$$

For the guns considered in Section 4.1 and a square-cell grid of period 0.55 mm and the transparency 0.8, the considered effect gives the additional normalized emittances are 0.35, 0.44, 0.64, 0.40 and 0.24 π mm·mrad respectively. In all the cases the effect of thinning out is much smaller than the ones of transverse inhomogeneity and of focusing in grid cells.

5. Conclusions

1. The emittance at the end of a space charge dominated circular-symmetric beamline can be reduced greatly if the parameters of the latter are optimized. Emittance compensation takes place for various current distributions of bunches and types of beam optics.

2. The compensation is strongest if the charge vibration phase advance through a beamline is $\approx 2\pi$. The value of emittance increases as n in $2n\pi$-minima. The values of emittance in $(2n+1)\pi$-minima are ever worse than in $2n\pi$ ones.

3. Longitudinal inhomogeneity typically stronger affects the emittance than transverse one. The combined effect is the strongest.

4. Lumped and distributed focusing produce almost equal effects.

5. The effect weakly depends on bunching and accelerating: as $v^{0.28...0.33}$ and $\alpha^{-0.136...0}$, where v and α are the bunching and accelerating coefficients.

6. The effect of longitudinal inhomogeneity is typically strongest in electron guns. The emittance from a gun can be improved significantly by adding an optimal compensation beamline.

7. Focusing in the grid cells usually weakly affects the emittance. This effect can be significant at peak currents lower than optimal one.

8. The two other effects in guns, scattering on a grid and thinning out, are apparently negligible.

References

[1] *I.M. Kapchinskii, V.V. Vladimirskii*. Proc. Int. Conf. on High-Energy Acc. and Instrum, CERN, Geneva, 1959, 274.

[2] *S.V. Miginsky*. NIM **A, 558** (2006), 127.

[3] *B.E. Carlsten*. NIM **A, 285** (1989), 313.

[4] *L. Serafini. J. Rosenzweig*. Phys. Rev. **E, 90** (1997), 7565.

[5] *S.V. Miginsky*. Minimization of Space Charge Effect. XVI International Synchrotron Radiation Conference SR-2006, Novosibirsk, Russia, 10-15 July 2006 (Proc. to be published in NIM).

[6] *S.V. Miginsky*. Optimal Beamlines for Beams with Space Charge Effect. - XX Russian Conference on Charged Particle Accelerators (RuPAC–2006), Novosibirsk, Russia, September 10-14, 2006, (Proc. in http://accelconf.web.cern.ch/accelconf/).

[7] *S.V. Miginsky*. Electron Guns and Beamlines in the View of Emittance Compensation. Asian Particle Accelerator Conference (APAC 2007), Indore, India , Jan 29 - Feb 2 2007 (Proc. in http://accelconf.web.cern.ch/accelconf/).

[8] *H. Bruck*. Accélérateurs Circulaires de Particules. Presses Universitaires de France, 1966.

[9] *L.D. Landau, E.M. Lifshitz*. Course of Theoretical Physics : Mechanics. Pergamon Press plc 1960.

[10] *J.R. Dormand and P.J. Prince*. SIAM J. Sci. and Statist. Comput., **10** (1989), 977-989.

[11] *S.V. Miginsky*. New Quadratures with Local Error Estimation and Two Strategies of Step Control in Calculation of Definite Integrals. Prepr. BINP #2001-18, Novosibirsk, 2001.
http://www.inp.nsk.su/activity/preprints/files/2001_018.pdf

[12] *S.V. Miginsky*. International Journal of Computer Mathematics, **80** (2003), #3, 347-356.

[13] *B.N. Pshenichny, Yu.M. Danilin*. Numerical Methods in Extremum Problems. Nauka, Moscow, 1975 (in Russian).

[14] *J.R. Pierce.* Theory and Design of Electron Beams, Van Nostrand, Princeton, New Jersey, 1954.

[15] *M.A. Tiunov, B.M. Fomel and V.P. Yakovlev*. SAM – an Interactive Code for Evaluation of Electron Guns, Budker INP prepr. 96-11, Novosibirsk, 1996.

[16] *S.V. Miginsky, V.V. Anashin, V.S. Arbuzov, et al*. Status of a 2-MeV CW RF injector for the Novosibirsk high-power FEL. Asian Particle Accelerator Conference APAC 2001, Beijing, China, September 17 - 21 2001. Proc.: 82.

[17] *V.F. Kozlov*. Handbook on Radiation Safety. Atomizdat, Moscow, 1977 (in Russian).

[18] *B. T. Price, C.C. Horton, K.T. Spinney*. Radiation shielding. London - New-York - Paris, 1957.

S.V. Miginsky

**Space charge effect,
coherence of charge vibration and emittance**

С.В. Мигинский

**Эффект собственного заряда,
когерентность зарядовых колебаний и эмиттанс**

ИЯФ 2007-11